Utrecht University

ARCADIS

MSc Graduation Research
Environmental Sciences | Water Science and Management

The effects of soil behaviour models on the reliability of stability calculations in 2-D LEM model for dikes in the Dutch context

Bas van Dijk
Student number: 3801063
Email: b.vandijk4@students.uu.nl

First supervisor: L.P.H. van Beek
Second supervisor: M.F.P. Bierkens
External supervisor: R. Koopmans

June 2019

Aerial photo on front page by R. Kruijt, water management and landscape specialist at Arcadis, October 2018.

B. van Dijk
MSc student Water Science and Management
Student number: 3801063
Email: bvandijk06@gmail.com
Utrecht University, the Netherlands

Utrecht University

First Supervisor
Dr. L.P.H. van Beek
Assistant Professor of Physical Geography
Utrecht University

Second Supervisor
Prof. dr. ir. M.F.P. Bierkens
Professor of Physical Geography
Utrecht University

External Supervisor
Ing. R. Koopmans
Senior Specialist Geotechnics
Arcadis Nederland

Preface

This thesis has been written in the interest of my graduation research for my Master's Water Science and Management at the University of Utrecht under the supervision of dr. Rens van Beek, and was performed in the context of an internship at Arcadis under the supervision of Ing. Rimmer Koopmans. Model input data partially originate from Ing. Leo Kwakman's dike reinforcement research at Wijk bij Duurstede and Amerongen, who is a water defence and geotechnical specialist at Arcadis.

First of all I would like to express my gratitude towards Rens and Rimmer. Rens, thank you for your inspiration and your feedback, your help with the probabilistic aspect, and your infinite guidance. Rimmer, thank you for letting me be part of the advisory group water safety at Arcadis, your trust in my competence for this research, and your supervision and persisting encouragement during the last five months. Secondly, I would like to thank Leo for his assistance with the kick-off of my research, and my fellow-Arcadians, Stef, Orin, Jelle, and Martin for sharing their knowledge and helping me out with several modelling issues.

Lastly, I am very grateful to my parents, Joke and Johan, my sisters, Janine and Nadie, my girlfriend, Di, and the rest of my family and friends for their boundless support during my studies.

Bas van Dijk

Utrecht, June 2019

Abstract

Thousands of kilometres of dikes cover the Dutch coastline and river shores, in order to protect the densely populated (hinter)land from high tide and floods. As a consequence of economic and demographic development, but also climate change, the safety and design standards of a flood defence need to be updated every fifty years or so. Macro-instability, which is the loss of structural integrity due to high water, is one of the significant failure mechanisms a dike must be evaluated for.

For this research a case study is assessed by means of a 2-D LEM (Limit Equilibrium Methods) model (i.e. D-Stability): for sixteen schematised dike sections that are part of the river dike between Wijk bij Duurstede and Amerongen (WAM) this programme is used to determine a stability factor. The geotechnical parameters (i.e. soil strength and volumetric weight) that serve as input for these calculations, have already been established by local field work and laboratory experiments (i.e. triaxial compression tests and direct simple shear tests). As the soil reacts differently depending on the stress it is exposed to, and therefore the sustained axial strain and deformation, different standards can be assumed. For this study three soil behaviour models are considered, i.e. Mohr-Coulomb (low axial strain), peak strength (maximum soil strength), and critical state (high axial strain).

As could be expected, the relatively high soil strength parameters for Mohr-Coulomb and peak strength result in much higher stability factors (average of respectively 1.9 and 1.7), than the ones for the conservative critical state (average of 1.3). This correlation has been confirmed by all case study results, comprising three selected sliding surface shape models (i.e. Bishop, UpliftVan and Spencer). The primary aim of this research was however not only to analyse these three different soil behaviour models, but also to find out which one is able to produce the most reliable dike macro-stability results. By virtue of the Probabilistic toolkit for each dike section and stability factor, concomitant reliability indices were calculated, which are established on the standard deviation of the geotechnical parameters. The relation between the stability factor and the reliability index is presented for each soil behaviour model. Based on only the results of this study case, there is no reason to favour any soil behaviour model over critical state when assessing dike macro-stability: for a significant stability factor it produces both the highest reliability index, and a much smaller uncertainty range. Due to the limited amount of soil samples, and even more important, the lack of heterogeneity of the geometry, lithology and geotechnical parameters, additional research is recommended, in order to obtain a complete overview of the relationship between stability and reliability, and to reduce the uncertainty that comes along with each soil behaviour model.

Contents

List of figures

List of tables

1 Introduction

1.1 Problem statement

Over half of the surface of the Netherlands is identified as highly susceptible to floods by either sea or rivers. A quarter is even located below the current sea-level (Slomp, 2012). Due to its geographical position the country has been struck by multiple extensive floods in the last centuries, of which the last one in 1953 was caused by a fierce storm surge that breached the coastal defences. This natural disaster induced a national development programme to raise the protection level offered (Huizinga, 2012). Nowadays almost eighteen thousand kilometres of dikes are established on the Dutch coastline and river shores to prevent recurrence of such events. Due to the high safety standards for the flood defences established by the national government, the Netherlands is even recognised as the safest delta in the world (Pieterse et al., 2009).

Dikes need to be managed and maintained constantly, and the safety levels and design criteria have to be revised regularly, on account of local economic and demographic development (Pieterse et al., 2009; Huizinga, 2012), but also in consideration of climate change, which is expected to prompt more extreme weather conditions in the (near) future. Forecasts indicate milder winters, warmer summers, longer periods of drought, more precipitation, more intense precipitation and a rising sea-level. As a consequence rivers will have to process more water and events of extremely high water-levels will be more frequent (RCE, 2013). Each of these factors may impact dike safety by increasing the external loads during floods and storm surges, or by decreasing the internal strength.

As a result of an extremely high water-level outwards of a river embankment, which induces a higher water stress both in the dike and subsoil, combined with other forms of stress (e.g. external burden or internal weakening), the structural integrity of the dike can decrease severely. An insufficient shear resistance (i.e. strength) of the soil can induce cracking, deformation of the soil, and local subsidence in the crest of the dike, which can all lead to the sliding of large parts of the dike's slope (Fig. 1.1) and ultimately the loss of a dike's flood defensive function. As a consequence the hinterland will become vulnerable for possible flooding. The impending failure mechanism that comprehensively defines these symptoms is called macro-instability, which is a phenomenon that can develop both at the inner and outer slope of the dike (van Duinen, 2015).

Macro-(in)stability is defined by whether the shear resistance of soil, which is dependent on friction, cohesion and the interlocking of particles, is sufficient to withstand disturbing forces and moments, including those arising from the weight of the soil mass above a likely shear zone. Loads that are imposed on the soil lead to strain, and by rearranging the soil particles, may feedback in the available shearing resistance. When the driving forces and/or moments continue to increase relatively and eventually surpass the maximum of available resisting

forces and moments, static equilibrium cannot be maintained and the soil will fail, in which case the soil deformation will accelerate unchecked under the net excess shear stress in theory. This deformation will concentrate in a narrow zone that constitutes the shear zone, and failure will manifest itself as a discrete sliding mass (van Duinen et al., 2016).

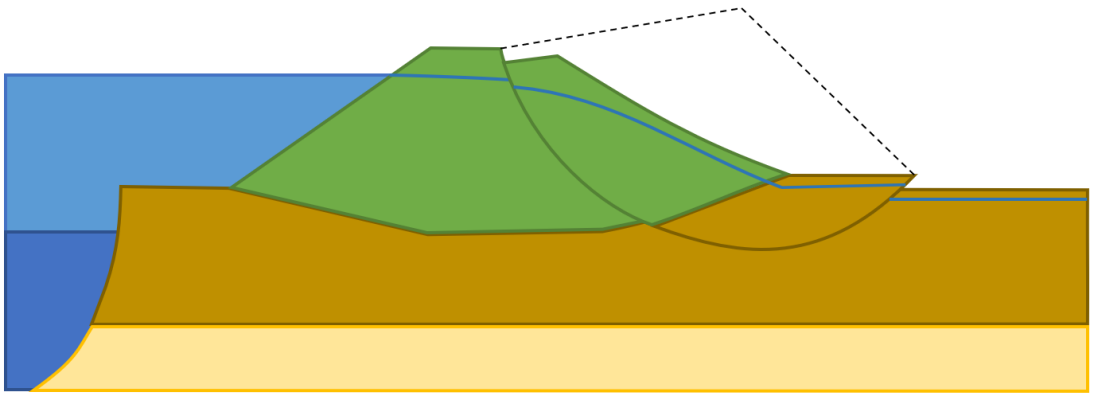

Figure 1.1: Inward macro-instability of a dike in which case a large part of the dike and subsoil slide off (van Duinen, 2015).

To describe the strain-dependency of the shearing resistance, different constituent soil behaviour models to quantify the soil strength can be defined. Typical curves for the behaviour of these models are presented in Figure 1.2, which can be derived from laboratory tests on soil samples. For loose sand or normally consolidated clay the deviator stress increases continually with an increasing axial strain until it reaches its critical state, and thus its ultimate strength, at which point there is no further change in volume or effective stress. Strain-dependent soil strength is particularly relevant for dikes as the soil material used is compacted during construction, and is compacted during construction: sand is compacted by means of vibratory rollers, and clay by a compactor/roller often fitted with a sheepsfoot drum. Due to the compaction through mechanical energy, soil particles are rearranged, which leads to a smaller total volume and a lower void ratio. As a result the shear strength is increased and the soil will deform less easily. This is graphically presented (Fig. 1.2) by a relationship with an increasing strain for an increasing stress until the peak strength is reached. Hereafter the maximum stress decreases (i.e. softening) until it reaches the critical state (van Duinen, 2015).

The complete stress-strain relationship is of significant value, as if one would rely on only one specific value, there is a considerable risk of misjudging the strength (Verruijt, 2001). With that in mind, it can be stated that when the ultimate strength is used, the additional strength achieved by soil compaction is completely neglected: for limited strain and deformation, the dike is truly stronger than assumed in critical-state-based assessment, which in theory would add safety to the design.

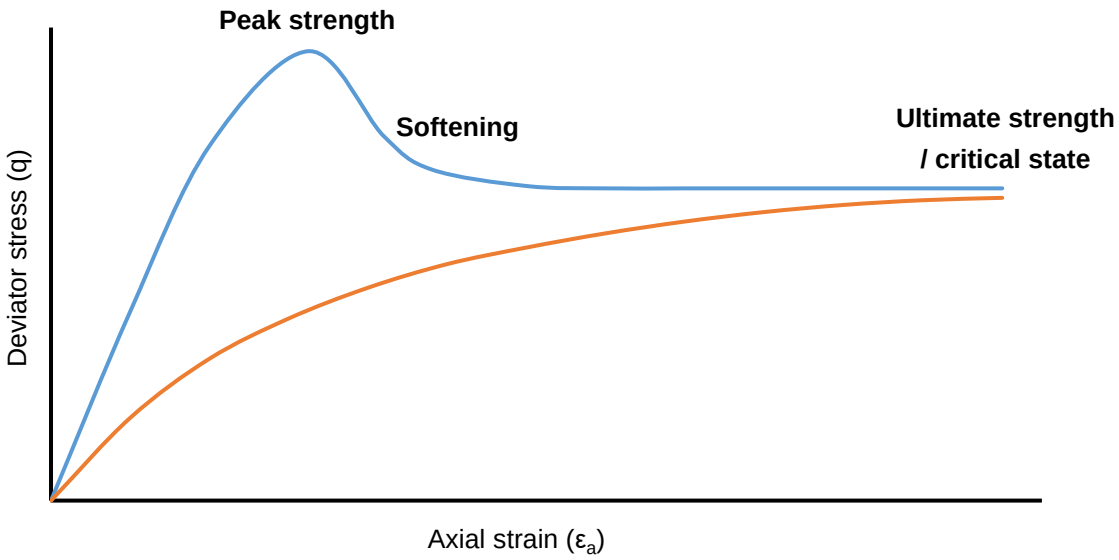

Figure 1.2: Standard outline of a stress-strain relationship for a loose or normally consolidated material (orange) and a dense or over consolidated material (blue) (van Duinen et al., 2016).

1.2 Research questions and objectives

In order to decide whether a dike must be considered as unstable, and needs to be reinforced, it must be evaluated for case-specific requirements for the probability of failure (i.e. the likelihood of macro-instability to occur). Generally such an assessment consists of four steps: 1. the collection of data, 2. the schematisation of it, 3. computation/modelling, and 4. the interpretation of the results (van Duinen et al., 2016). The modelling and evaluation procedure currently assesses dike stability through three progressive tests: an elementary test ("eenvoudige toets"), a detailed test ("gedetailleerde toets") and a customised test ("toets op maat"). These tests are listed here in ascending order of accuracy and detail (de Waal, 2016).

The elementary test only evaluates the dike on general characteristics and standards, and is merely intended to identify dikes that are evidently safe. If not, the evaluation is to be continued by a detailed test, and possibly also a customised test, for which stability calculations are carried out by a 2-D LEM (Limit Equilibrium Methods) model, and the required probability of failure is tested by means of probabilistic or semi-probabilistic models (de Waal, 2016).

The assessment of dike macro-stability is currently established on the soil's ultimate strength (i.e. the critical state soil behaviour model), which is considered as quite conservative and accompanied by a certain safety margin. The primary objective of this research is to examine whether using the peak strength is preferred over using the ultimate strength, when assessing the macro-stability of a dike, assuming a normative high water-level. A third soil behaviour model is also analysed throughout this study to give more insight of the process: Mohr-Coulomb, which is based on a small amount of axial strain and used to be the conventional

method until the start of 2017. In order to achieve the primary objective, a number of research question have been formulated to structure the research process:

1. How do the geotechnical parameters, which represent the soil strength in stability calculations, compare for each soil behaviour model?
2. What is the fundamental influence of the parameters and the drained/undrained soil conditions for each soil behaviour model on the stability and reliability?
3. Will the implementation of the peak strength, rather than the critical state, lead to more stability, and is it equally reliable under imposed loads?
4. What is the effect of the slope and predominant soil type of the dike on the macro-stability?

The answers to these questions are of significant value, but have not yet been given, since the recent shift in the normative soil behaviour model, and the lack of experience with the design of a dike based on the peak strength. As the safety margin is lost, when not working with the ultimate strength, the safety requirements must be set higher, where the critical stability factor is the great unknown. A potential outcome of the research is that the peak strength can be associated to an increase in the shear resistance, which means that dikes are actually stronger than as assessed by the critical state soil behaviour model: unnecessary dike reinforcement could be prevented.

A case study will be considered (section 1.3), in order to reach the primary objective, and to solve the presented research questions, by means of an applied and comprehensive macro-stability assessment executed for each of the selected soil behaviour models. The findings of this research will be of significant interest to the Dutch engineering practice and could possibly be incorporated into existing procedures and models.

1.3 Case study: WAM

The flood risk of a dike is primarily dependent on the local population density, companies/industry and vital infrastructure. For the fluvial area in the centre of the Netherlands a possible dike breach could lead up to €16 billion in expenses. A large part of the Dutch megalopolis the Randstad could become submerged, with almost half a million people directly affected (de Bruijn & van der Doef, 2011). In order to have the primary flood defences meet the constantly increasing safety levels, the waterboard “Hoogheemraadschap De Stichtse Rijnlanden” (HDSR) started with the reinforcement of the dike along the Lek river in 2017, which is part of the national high water protection programme (“Hoogwaterbeschermings-programma”: HWBP).

During the first stage of the Lek dike reinforcement project, subproject WAM is considered, of which the reconnaissance phase has already started in 2017. WAM stands for *Wijk bij*

Duurstede and Amerongen and defines the 11 kilometre-long dike trajectory between these two towns (Fig. 1.3). During the first stage of the subproject, the dike has already been analytically assessed for the prospective safety requirements on piping (i.e. groundwater in a permeable soil layer below the dike carries away sand), inward macro-stability (based on the critical state soil behaviour model), and its height. These three failure mechanisms control the safety statement, which was disapproved at the time, as approximately 90% of the length of the dike trajectory does not meet the fixed requirements (Sweco & Arcadis, 2018). Piping has been determined as the most impending safety risk. Macro-instability was determined to be a threat mainly alongside Wijk bij Duurstede and the agricultural lands in the centre. To develop and test this study's model, WAM and its available data will serve as a case study, as test results from other dike reinforcement projects are still scarce.

As field data was limited and the safety statement came with a considerable uncertainty range, additional fieldwork and laboratory research were necessary in order to increase the information on the structure and composition of the subsoil for setting up lithological cross- and longitudinal profiles, and to determine the relevant geohydrological and geotechnical parameters. These have been achieved in 2018 by the execution of cone penetration tests (CPTs), ground drillings, placing groundwater monitoring well pipes and stress meters, and carrying out laboratory tests (i.e. compression tests on cohesive soil samples). The soil was found to consist mainly of fluviatile clay and sand: a top layer of weak sandy clay, sporadically followed by a layer of peat bog, a relatively thick layer of strong sandy clay, and the foundation is consistently composed of a solid and packed sand layer (Hertogh & Stellema, 2018).

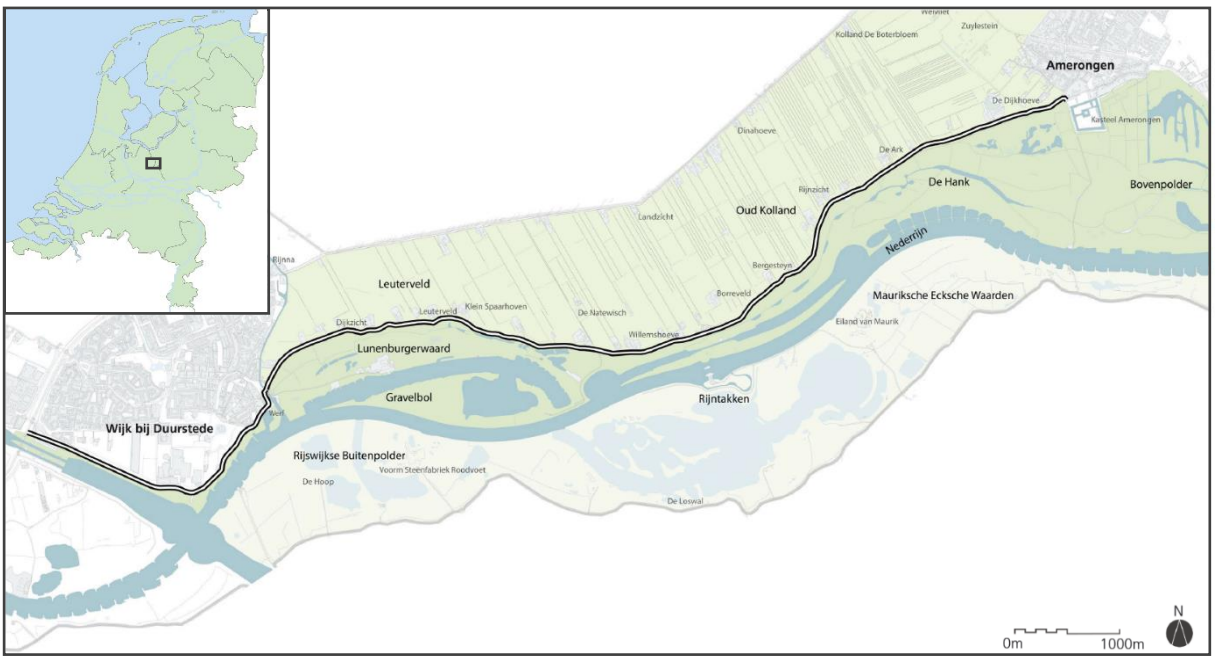

Figure 1.3: Geographical map of case study area: the river dike between Wijk bij Duurstede and Amerongen (Sweco & Arcadis, 2018).

2 Theory and background

2.1 Shear strength soil mechanics

The shear strength, which acts as the resistance against soil instability, is not a constant: as mentioned before it can be defined by a stress path, or a certain stress-strain relationship (Fig. 1.2), where the stress, q (kPa), is plotted against the axial strain, εa (-). Three soil behaviour models are distinguished:

- Mohr-Coulomb, the soil strength assuming 2% of axial strain.
- Peak strength, the maximum measured soil strength for an undefined amount of strain.
- Critical state (or ultimate strength), soil strength for a large strain percentage (25%) and maximum deformation.

The mathematical model that has always been used to describe soil mechanics in response to shear stress is the Mohr-Coulomb theory (Coulomb, 1776; Řeřicha, 2004), for which the drained shear strength is proposed to be a combination of adhesion and friction components:

$$\tau_f = c' + \sigma_f' * \tan \phi \qquad \text{(Schofield, 2006)} \qquad 2.1)$$

where

- τ_f is the shear stress on the sliding surface for saturated soil (kPa)
- c' is the cohesion: cannot be directly derived from the laboratory tests, but in general rather is the result of extrapolation of drained measurements. As the sources of cohesion can be diverse and highly variable, the parameter itself can vary considerably as well (kPa)
- σ_f' is the effective normal stress on the sliding surface: the normal stress minus the porewater pressure (kPa)
- ϕ is the angle of internal friction: the effective shear strength for drained soil behaviour, defining the degree of friction between soil particles (°)

For a drained stability analysis, the shear strength along the sliding surface is determined by the effective normal stress at the base of the sliding surface. For a circular sliding surface this is expressed by substitution of the vertical equilibrium of the force acting on the sliding surface in equation 2.1:

$$\tau_i = \frac{c_i + \sigma_{vi}' * \tan \phi_i}{1 + \tan \alpha_i * \tan \phi_i / Y} \qquad \text{(Deltares, 2017)} \qquad (2.2)$$

where

- τ_i is the shear stress at the bottom of the sliding surface i (kPa)

- c_i is the cohesion at the bottom of the sliding surface (kPa)
- σ_{vi}' is the vertical effective stress at the bottom of sliding surface (kPa)
- ϕ_i is the internal friction angle of the soil at the bottom of the sliding surface (°)
- α_i is the angle at the bottom of the sliding surface (°)
- Y is the stability factor (-)

Cohesion, which defines the attraction force between soil particles as a consequence of electromagnetic binding, cementation and/or over consolidation, is not a fundamental soil property however: today the Critical Soil State Mechanics (CSSM) theory is preferred in Dutch practice, which in contrast to the first, does consider deformation before, during and after the soil failure mechanism (Schofield & Wroth, 1968). Hence, the shear stress is only determined by the effective normal stress and the critical state friction angle. A crucial interest of the critical state soil behaviour model is that it is able to distinguish soil types with a high permeability, which are coupled to drained soil behaviour, from soil types with a low permeability, which are coupled to undrained soil behaviour (van Duinen, 2014):

$$S_u = S * \sigma_v' * OCR^{\,m} \qquad \text{(Zwanenburg et al., 2013)} \qquad (2.3)$$

where

- S_u is the shear strength for undrained soil behaviour, (kPa)
- S is the shear strength ratio (-)
- σ_v' is the effective vertical stress (kPa)
- OCR is the over consolidation rate: defines a ratio between stresses, therefore it is dimensionless (-)
- m is the strength increase exponent: a parameter that defines the degree of the effect of pre-burden (i.e. yield stress and OCR) on the undrained shear strength (-)

The shear stress acting at the bottom of a sliding surface is assumed as equal to the specified value for the undrained strength.

For POP (pre overburden pressure) = 0, OCR = 1 and m = 1.0, due to the following relation:

$$\sigma_p = \sigma_v' + POP \qquad \text{(Zwanenburg et al., 2013)} \qquad (2.4)$$

where

- σ_p is the yield stress (kPa)
- σ_v' is the effective vertical stress (kPa)
- POP is the pre overburden pressure (kPa)

The yield stress defines the soil condition (i.e. the sedimentation environment and the degree of pre-burden of the undrained soil), which is either expressed as normally consolidated or over consolidated: meaning with respectively a low or high packing density of soil particles. It is a geohydrological parameter that can show a lot of variation, both local and regional, and therefore it can only be carefully estimated without local field research. In order to get an accurate interpretation, relevant characteristics are derived from available CPTs and compression tests.

The relation between the first two factors is defined as the *OCR*, which is directly correlated to the shear strength of undrained material. For the POP, which serves as an auxiliary arithmetic parameter, conservative, but optimised standard values are normally assumed (van Duinen, 2016).

Currently the ultimate strength is used for establishing the soil strength parameters (van der Veen et al., 1981; Crabb & Atkinson, 1991; van Duinen et al, 2016) that serve as input for the LEM model. By adopting the ultimate strength, the implicit assumption is made that the shear strength is mobilised (i.e. the soil contributes to the slope's stability) along the entire sliding surface (van Duinen, 2015). Although this is confirmed by an abundance of study cases (Larsson, 1980; Terzaghi et al., 1996), a considerable amount of deformation is needed at the bottom of the sliding surface (i.e. the passive zone) for full mobilisation of the shear strength, while only limited deformation of the slope is sufficient for the mobilisation of the peak strength at the top of the sliding surface (i.e. the active zone). This correlation is a direct consequence of anisotropy of the soil stress state (van Duinen, 2015).

The peak strength is promised to give the greatest soil strength at the moment of macro-stability failure. This is partly due to a greater value for the friction angle, and the presence of cohesion, but it also brings about an interlocking contribution: the measure of deformation and axial strain is considerably smaller for peak strength, but also Mohr-Coulomb, resulting in dilatancy, which is an increase in volume by shearing and results in a professed additional strength, caused by a decrease of water stress in saturated soil (van Duinen et al, 2016).

2.2 Description of research process

Ground drillings, cone penetration tests and groundwater monitoring

The information that is derived from ground drillings, which can be executed both manually as mechanically, is together with data obtained from CPTs indispensable for establishing the composition and structure of the dike. By means of these methods of research it is possible to determine specific soil layer characteristics such as the volumetric weight of the soil, γ, which is easily determined through the weight and volume of soil samples obtained by ground

drillings, and the water stress that will ultimately result in an accurately schematised subsoil model.

Ground drillings are mainly executed for the purpose of classification and identification of the subsoil, which are generally based on visual description of the collected samples and verified by laboratory tests (TAW, 2001) (Appendix A). The results that follow from ground drillings typically form the basis of the soil-mechanical analysis. In order to achieve reliable parameters, both the quality and quantity of soil samples acquired by ground drillings need to be sufficient. At least two points of measurement have to be taken over the width of the dike, of which one located in the crest of the dike and one in the hinterland, to get an accurate definition of the soil conditions (van Duinen et al., 2016).

CPTs are mainly carried out in order to determine the soil composition (i.e. layer structure), by measuring the cone resistance and the skin friction, however the results are also able to indicate the yield stress and the undrained shear strength through correlations (van Duinen et al., 2016) (Appendix B). Currently the Deltares CPT-tool is used to define the geotechnical data that is extracted from the field. The user-defined interpretation model within this tool is able to classify up to 14 different soil types from CPT data and ground drillings (Deltares, 2016).

Groundwater monitoring well pipes and stress meters are often placed at the site of the CPTs and ground drillings, in favour of an unambiguous registration of the phreatic level, which is the unstrained groundwater level that represents the position within the subsoil at which the water pressure is equal to the atmospheric pressure (Verruijt, 2001; van Duinen, 2016). Herewith one must account for the influence of variable burdens (e.g. precipitation, outside water level) on the water pressure (Zwanenburg et al., 2013).

Triaxial compression tests

Both the drained and undrained shear strength parameters can be determined by a triaxial compression (TC) test of the cylindrical soil samples that are obtained by ground drillings. During the strain-controlled test, the sample is confined between two rigid plates and enveloped by a rubber membrane. The whole is placed in a cell that is filled with a liquid, which is pressurised, thereby exerting a constant power equal to the cell stress on the membrane, both vertically and horizontally (Visser et al., 1988), where the degree of stress is dependent on the geotechnical point at issue and the stress level in-situ (van Duinen et al., 2016). This process induces a change in the length of the soil sample (i.e. deformation), which is correlated to the axial strain of the soil as follows:

$$\varepsilon_a = \Delta h_b / h_c \qquad \text{(NEN, 1992)} \qquad (2.4)$$

where

- ε_a is the axial strain (%)

- Δh_b is the difference in the length of soil sample during the process (mm)
- h_c is the length of the soil sample after consolidation (mm)

This consolidated pressure test with an imposed axial-symmetric stress state enables one to identify the relevant geotechnical characteristics of an unaffected soil sample (Appendix C), where the soil strength parameters or the shear resistance are derived from the deviator stress.

These tests are executed for a collection of samples representing different soil layers, depths and drilling locations that results in a set of data presenting the shear strength for different stress levels (Zwanenburg et al., 2013). Together with the DSS test, this test is considered to give the most accurate and comprehensive rendition of stress deformation behaviour within subsoil (CUR, 1992).

Direct simple shear tests

While TC tests are used to represent the behaviour of clay within a sliding surface, direct simple shear (DSS) tests are considered for peat bog, as the first will give unrealistically high shear strengths due to the material's texture. No radial or vertical pressure is exerted for this type of test: only the horizontal shear strength is measured for a gradually increasing shear stress (van Duinen et al., 2016).

Schematisation of the subsoil

Based on the data achieved by local soil research (i.e. ground drillings and CPTs) and available lithological and elevation maps (of the wider area), it is possible to draw up a detailed subsoil schematisation that covers the depth and extent of every soil layer within the dike area, for which geotechnical parameter values will be assigned by means of the results from laboratory tests. The schematisation is a very important component of the soil mechanical assessment of a flood defence, and placed in the centre of the process (Fig. 2.1): optimisation is only possible when sufficient local data is available, as the composition of the subsoil can vary greatly on a relatively small scale (van Duinen et al, 2016). The effect of uncertainties within the schematisation is claimed to be at least equivalent to the effect of uncertainties based on the geotechnical characteristics. Currently a so-called schematisation factor is used to deal with the uncertainties throughout: this partial stability factor is primarily penalised for the limited availability of data and assumptions made (Zwanenburg et al., 2013).

Modelling of the sliding surface and probabilistic-stability calculations

Through a LEM model it is possible to determine the potential sliding surface that is most likely to occur, which is linked to a stability factor, *Y*. Most models used for these calculations assume a circular sliding surface of the dike slope (Fig 1.1) according to the Bishop model (Bishop, 1955), which is globally confirmed by empirical observations (van der Veen et al., 1981; Visser et al., 1988; Verruijt, 2001). However, for various conditions, the critical sliding surface can be

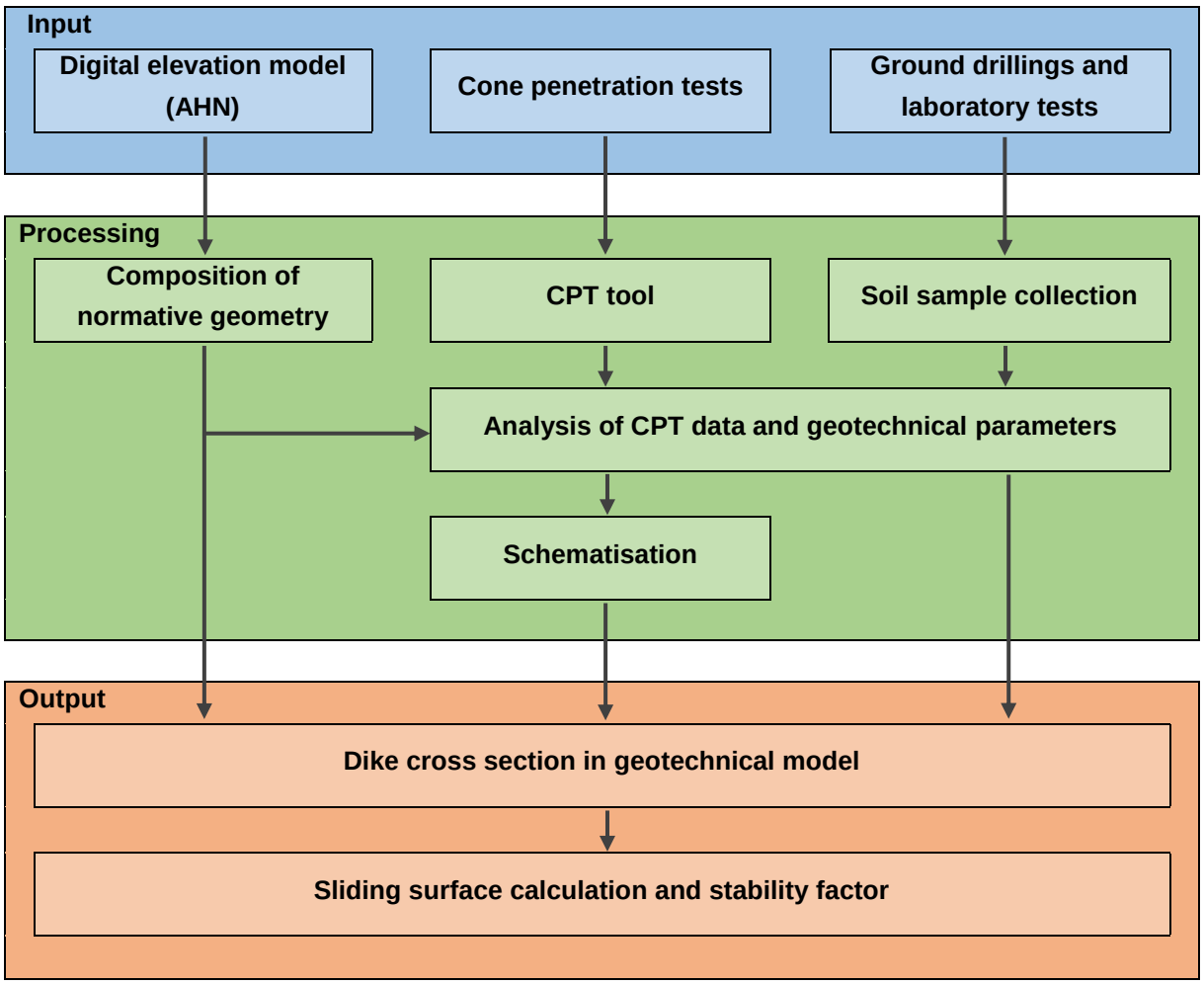

Figure 2.1: Flow diagram presenting the process of schematisation and the assessment of dike macro-stability in a LEM model.

non-circular. Acknowledged alternatives are the Spencer-van der Meij model (hereinafter referred to as 'Spencer') (Spencer, 1967; van der Meij, 2012) and the UpliftVan model (Van, 2001). These two models target sliding surfaces that can be both circular or follow partially horizontal lines, which can occur due to relatively weak soil layers (van Duinen et al, 2016). Therefore they do not only account for moment balance and a vertical balance of forces, but also for the horizontal forces within the sliding surface. Where the UpliftVan model is limited to a format of two circular segments connected by a horizontal plane, the Spencer model is in theory able to determine any sliding surface associated to the least shear resistance.

The type of sliding surface shape model that is employed must be accounted for when establishing the minimum required stability factor of a dike. This is done by including a so-called model factor, γ_d (-), which is dependent on the restriction in sliding surface shape of each method. This is not the only partial factor that the minimum required stability factor is controlled by however:

$$\gamma \geq \gamma_{min} = \gamma_b \cdot \gamma_d \cdot \gamma_n \cdot \gamma_m \qquad \text{(Bakker et al., 2011)} \qquad (2.5)$$

where

- Y is the calculated stability factor (i.e. output LEM)
- Y_{min} is the minimum required stability factor (does not need to be 1.0)
- Y_b is the schematisation factor (based on scenario's)
- Y_d is a standard model factor (Uplift Van: 1,06; Spencer: 1,07; Bishop: 1,11) (van Duinen et al., 2016)
- Y_n is the damage factor (based on the chance of failure and the design requirements)
- Y_m is the material factor

A value is associated to each partial factor based on the available data.

Subsequently a reliability index, β, can be calculated by means of a probabilistic model, which resolves the sensitivity and bandwidth of a model, given the uncertainties in the input parameters. The calculated index must be higher than the required reliability index, which is dependent on the required probability of failure: a value primarily based on the dike dimensions and the permitted probability of flooding (van Duinen et al., 2016). The reliability index is normally in the range of 4 - 6 for a primary flood defence.

2.3 Earlier research on WAM

For the case study of WAM six different soil types have already been distinguished:

- Top layer – anthropogenic dike material
- Clay – anthropogenic heavy, unsaturated dike material
- Clay – heavy (i.e. large volumetric weight)
- Clay – light (i.e. small volumetric weight)
- Peat bog
- Rounded, moderately sorted, well graded quartz sand

The distinction has not been based on the type of deposition (i.e. anthropogenic/natural), but rather on the cone resistance, water stress, and whether the soil is assumed as permanently saturated or not, as these factors prove to be most significant for the shear strength of the soil. The different types of clay are furthermore distinguished by their volumetric weight, POP, and geological position (Kwakman, 2019).

The schematisation that followed, which serves as input for the LEM model and the macro-stability calculations, is displayed as a set of cross sections of the dike and the subsoil, including the layer structure, the different soil types and their characteristics, and the water stresses. Due to severe heterogeneity in the subsoil, the schematisation is normative, and only representative for a segment of the flood defence: a dike section (Zwanenburg et al., 2013).

Depending on the length of the dike trajectory, and variability in lithology and geometry, the dike is subdivided into multiple sections, which are assumed to be homogeneous, and characteristic for the entire longitudinal scope of the section.

Four of twenty dike sections were considered as evidently safe due to a construction or the geometry, e.g. considerably wide dike crest. The remaining sixteen different cross sections have been evaluated (Tab. 2.1): these define the normative geometry and lithography for one dike section, and will altogether be representative of variety in circumstances over the length of the entire dike. The heterogeneity of the subsoil is schematised, where the layer composition and the dimensions are based on local ground drillings and CPTs.

Table 2.1: Overview of dike section division, including the dimensions and characteristics.

Dike section (#)	Start (DP m)	End (DP m)	Normative geometry (DP m)	Section length (m)	Altitude crest (m)	Altitude hinterland (m)	Slope (-)	Characteristic
1	0	1+5	n/a	76	10.8	7.5 - 8.5	1:2.5	High hinterland
2	1+5	14+60	12+65	1668	10.8	5.0 - 6.5	1:3.0	Gentle slope
2a	14+60	17+95	14+85	35	10.8	5.5	1:2.5	House behind dike
3	17+95	34+20	23+15	1625	10.8	4.5 - 5.5	1:3.0	Descending bank
4	34+20	39+30	36+15	502	10.4	4.5 - 5.5	1:3.0	Gentle slope
5	39+30	42+40	41+70	270	10.2	4.5 - 5.0	1:3.0	Wide crest
6	42+40	43+75	43+20	682	10.1	4.5 - 5.5	1:2.5	Small bank
6a	43+75	50+20	44+00	72	10.1	5.0	1:2.0	House behind dike
7	50+20	61+45	58+65	1129	10.0	4.0 - 5.0	1:3.0	Ditch behind dike
8	61+45	72+25	72+20	1078	10.3	4.5 - 5.5	1:3.0	Small bank
9	72+25	74+50	73+70	229	10.1	4.0 - 5.0	1:2.5	House behind dike
10	74+50	79+45	80+10	1032	10.3	4.5 - 5.0	1:3.0	Buildings & ditch in far hinterland
10a	79+45	85+40	79+90	62	10.3	5.0	1:2.0	House behind dike
11	85+40	85+55	n/a					Inlet sluice Kromme Rijn – construction
12	85+55	86+90	85+60	132	10.2	5.0	1:2.0	City line Wijk bij Duurstede
13	86+90	86+335	n/a					Beermuur Wijk bij Duurstede - construction
14	86+335	92+60	90+50	339	10.4	4.5 - 6.0	1:2.5	Altitude hinterland varies strongly
15	92+60	96+35	95+00	385	9.6	4.5	1:3.0	Highly heterogeneous geometry
16	96+35	99+130	n/a	473	10.0	4.5 - 5.0	1:2.5	Wide crest
17	99+130	105+95	104+80	897	10.0	4.5 - 5.0	1:2.5	Uniform geometry

The schematised dike sections in combination with the geotechnical data (established from the laboratory tests), where the 5% lower limit of the soil strength parameters is assumed, served as input to a LEM model. The stability factors that followed, can be compared to the minimum required stability factors, as introduced in section 2.2: the first needs to be larger or equal to the latter in order to authorize a dike as macro-stable. Kwakman (2019) established minimum required stability factors of 1.36, 1.38 and 1.43 for respectively the UpliftVan, Spencer, and Bishop shape model. Nine of sixteen dike section have been assessed as

unstable (Fig. 2.2). The degree of calculated failure can be expressed as the difference between the minimum required and the calculated stability factor, which varies from -0.04 to -0.29 (Kwakman, 2019).

The reliability has not been tested by a probabilistic model, but is simply determined by an empirically-based correlation introduced by van Duinen et al. (2016): $Y = 0.15\beta + 0.41$. This equation is able to quickly give an approximation of the reliability index, based on the calculated stability factor. This standard guideline is however only accurate for the critical state behaviour model, in combination with *characteristic* values for the soil strength parameters.

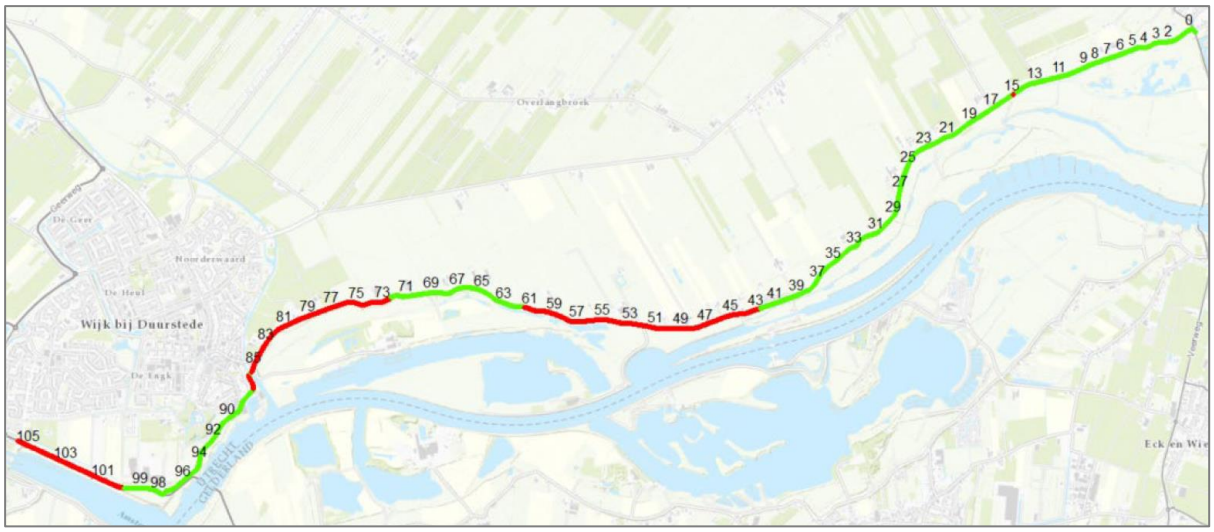

Figure 2.2: Inward macro-stability assessment of the WAM river dike for a normative high water level (numbers represent dike poles (DPs)).

3 Methods

3.1 Soil behaviour and geotechnical parameters

Before the critical state soil behaviour model was introduced as the standard for the mobilised shear strength in the interest of dike macro-stability evaluation in the legal assessment instrument (WBI) (de Waal, 2016), Mohr-Coulomb has always been considered as most adequate. Currently the latter is particularly argued for its lack of distinction between drained and undrained soil behaviour however. A still-unexplored alternative approach is considering the peak strength (of the undrained or drained shear strength, depending on the soil type, in the active part of the sliding surface) as the normative soil strength.

For the three soil behaviour models that are assessed during this study, the following assumptions are made:

- Mohr-Coulomb: the friction angle, ϕ, cohesion, c', and dilatancy are considered as to be representative for the soil behaviour for all material types. The little amount of strain induces drained soil behaviour. Moreover only soil samples that are associated to *OCR* > 1 (i.e. a high effective stress) are included for the parameter diversion, as laboratory tests with *OCR* = 1 are executed at a degree of pressure that cannot occur in the field with 2% strain.
- Peak strength: the friction angle, cohesion and dilatancy define the shear strength for the top layer, as fully remoulded soil behaviour does not yet occur. The different types of clay and the peat bog are assumed to be characterised by the shear strength ratio, *S*, and the strength increase exponent, *m*. For the latter the values are equivalent to the ones derived for the critical state, as the state of the ground (i.e. the yield stress, *OCR*, and *POP*) is not different as well. As also for the critical state, the distinction between drained and undrained soil behaviour is mainly based on the permeability: in a soil type such as sand, which is linked to a relatively high permeability, drainage can occur during dike macro-instability: for clay and peat bog, which have a low permeability, no to little drainage will occur (van Duinen et al., 2016).
- Critical state: the friction angle is considered to represent the soil strength of the top layer, while the shear strength ratio and the strength increase exponent are linked to the remaining materials. Cohesion and dilatancy are assumed to be negligible when calculating with the ultimate strength due to the large amount of strain/deformation.

A design value of 30° for the friction angle, as suggested by van Duinen et al. (2016), and also employed by Kwakman (2019), is assumed for sand due to its reliable stability, regardless of the soil behaviour model.

The sample collection tool presented by Kwakman (2019) is able to put a value to the relevant geotechnical parameters for each soil behaviour model, and each soil type: the tool is based

on all the available field and laboratory research data obtained for the case study WAM. The test results have already been analysed, during which erroneous ones were removed from the collection for varying reasons (e.g. a dubious consolidation phase, a doubtful course of the water stress or the deviator stress, or heterogeneous material). The newly-derived parameters have been validated by the CPT data: the shear strength and yield stress from both sources are matched. As an example, Figures 3.1a-b present the shear strength relations of heavy clay for drained (left) and undrained (right) soil behaviour (including the uncertainty presented by the 5% lower and upper limit).

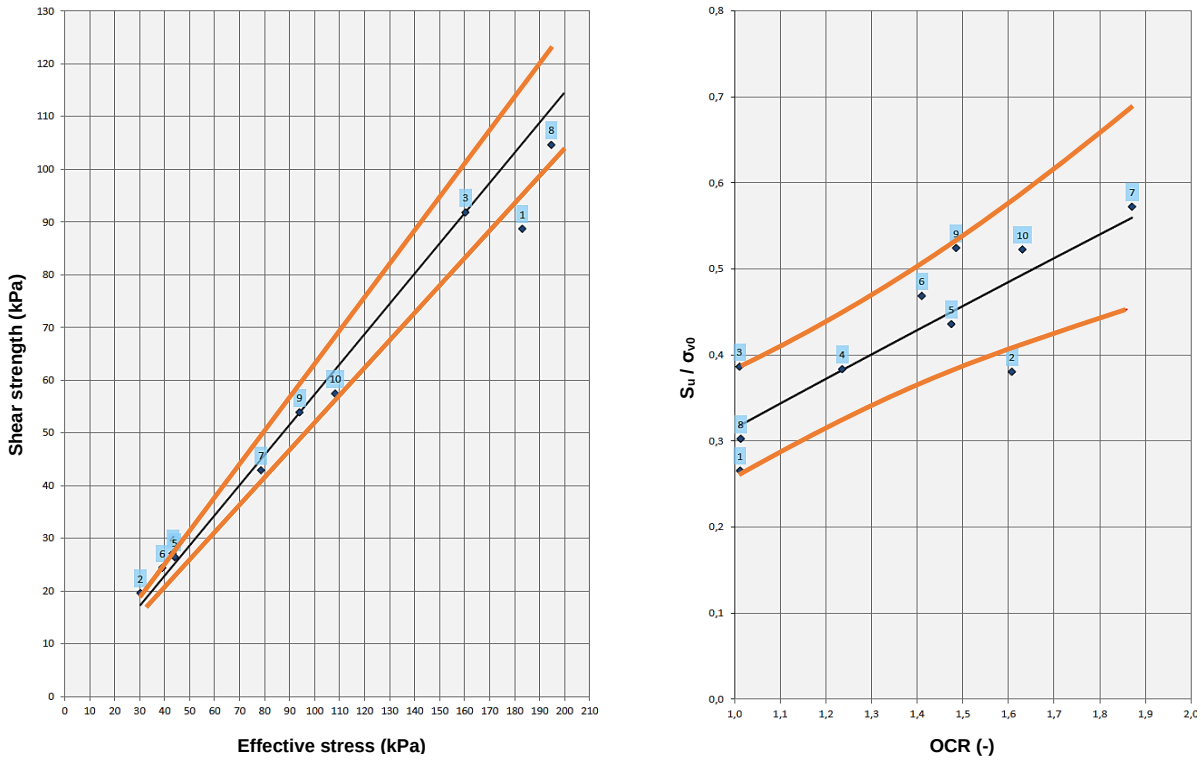

Figures 3.1a-b: Example of the shear strength analysis of heavy clay from the soil sample collection tool: the relation between the effective stress and the drained shear strength (left), and the undrained relation between the derived S_u-ratio for the soil samples and the degree of OCR (right). Black defines the expected value extracted from the (in this case) 10 soil samples, orange represents the 5% lower and upper limit.

Where the derived parameter values for drained soil behaviour have been assumed as trustworthy (based on accepted standard values), one of the two undrained soil strength parameters, the strength increase exponent, *m*, presented a false relation for the clayey dike material (sample size, *n* = 19): a value of 1.4-1.5, which physically cannot be higher than 1.0. This specific material does not show soil behaviour as recognised by the Stress History And Normalized Soil Engineering Properties (SHANSEP) material model: the soil samples present significantly high water stresses for little deformation, and subsequently decrease rapidly, which has been observed before by Janssen (2018). This is presumably caused by not entirely undrained soil behaviour and/or incomplete saturation. A standard value of 0.95 was assumed

alternatively. In contrast, the *m* for peat bog (*n* = 6) was considerably underestimated: 0.50-0.60. This was probably due to a limited amount of soil samples and soil heterogeneity. Default values of 0.80 have been applied. Following the sample collection tool heavy clay (*n* = 10) and light clay (*n* = 21) were linked to respectively 0.95 and 0.87 (Kwakman, 2019).

It has to be noticed that the geotechnical parameters established by Kwakman (2019) are only valid for the critical state soil behaviour model, and moreover represent the *characteristic* values (i.e. the 5% lower limit), which is assumed to be safer, however also more conservative. For this research the *expected* value of the soil strength parameters will be derived, as well as the concomitant uncertainty, expressed as the standard deviation, which is based on the scatter of the data points. The latter is latter is mainly in interest of the reliability analysis in the probabilistic model.

3.2 LEM model

The sets of soil strength parameters for all three soil behaviour models (i.e. Mohr-Coulomb, peak strength, and critical state), in combination with the schematised cross sections will serve as the input for the next step: by means of a LEM model (D-Stability: slope stability software for soft soil engineering by Deltares), which is based on a calculation procedure that is validated by eleven completely-monitored cases of macro-instability in the Netherlands (van Duinen, 2010; van Duinen, 2013), the macro-stability of the dike sections will be evaluated. Just as Kwakman (2019), for the analysis of macro-stability the normative high water level ("maatgevende hoogwaterstand") is assumed, which is based on the legal maximum design discharge, which is determined by the Generator of Rainfall and Discharge Extrems (GRADE) (Hegnauer et al., 2014) for the Lek river.

Through the geotechnical two-dimensional model, which consists of generalised soil mechanics, it is possible to submit reality to hypothetic, but probable circumstances for the benefit of assessment. In order to do so for the evaluation of dike macro-stability, the failure mechanism is imposed within the model before the actual calculations, rather than derived from the calculations. In short, the ratio between the strength and the burden/load is algorithmically determined for multiple potential sliding surfaces derived from tangents through a grid of possible midpoints (van Duinen et al., 2016).

The failure mechanism is also tested for three different shapes of sliding surfaces by a limit equilibrium method (i.e. Bishop, UpliftVan, and Spencer). The stability factor of a two-dimensional soil structure will be algorithmically determined for each one, alongside an arbitrary shape and orientation, with the purpose of studying the correlation, and serving as a validation of each other (Fig. 3.2a-c). The kinematically possible sliding surface with the lowest stability factor is considered as normative: if the failure mechanism is proven not to occur, the dike slope can be considered as stable (Visser et al., 1988).

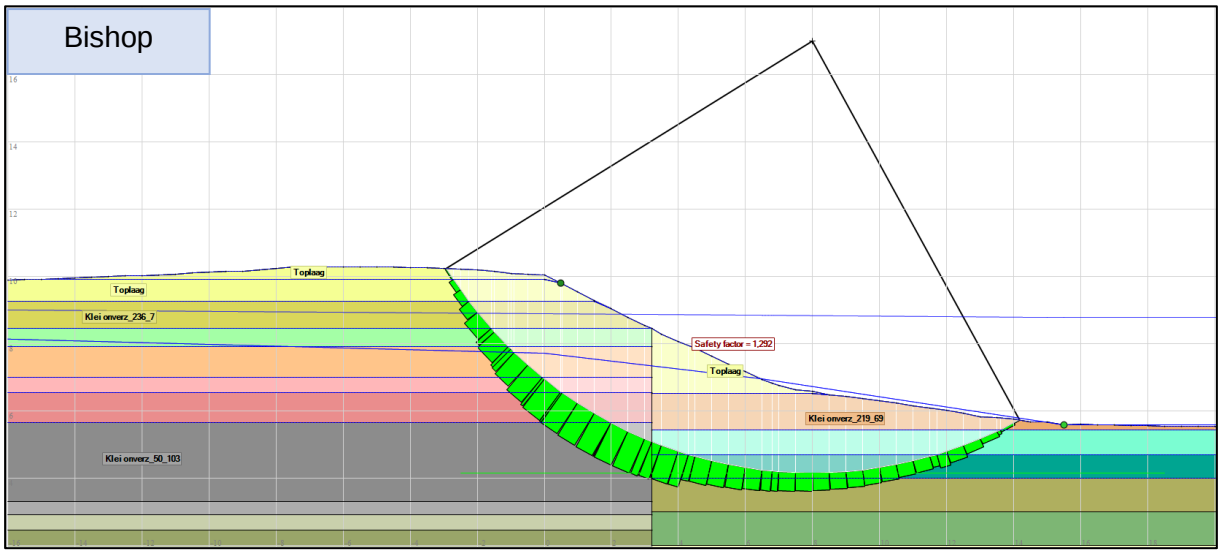

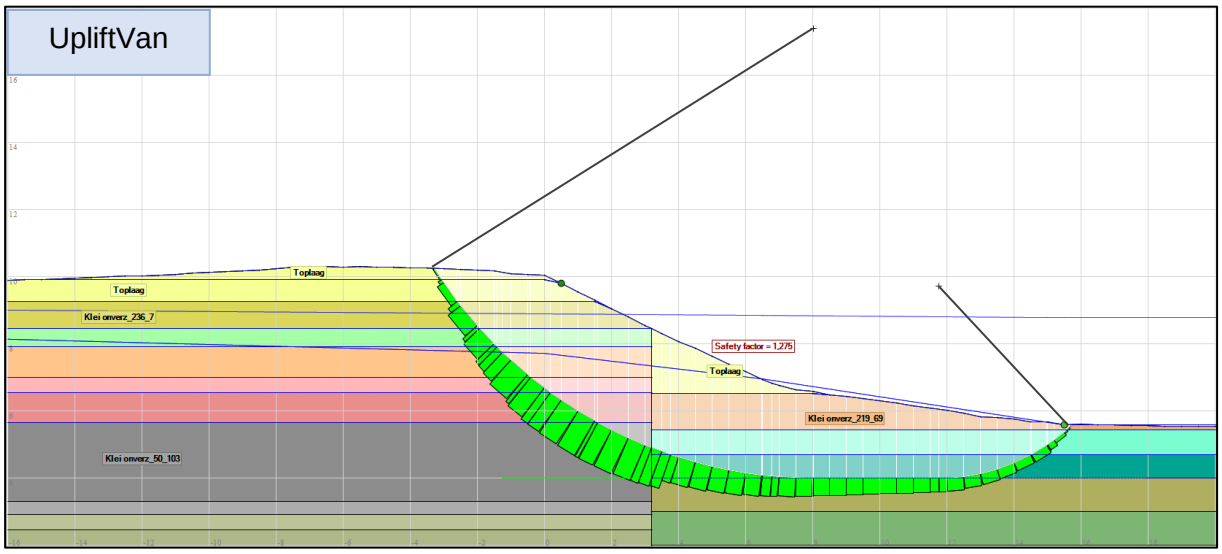

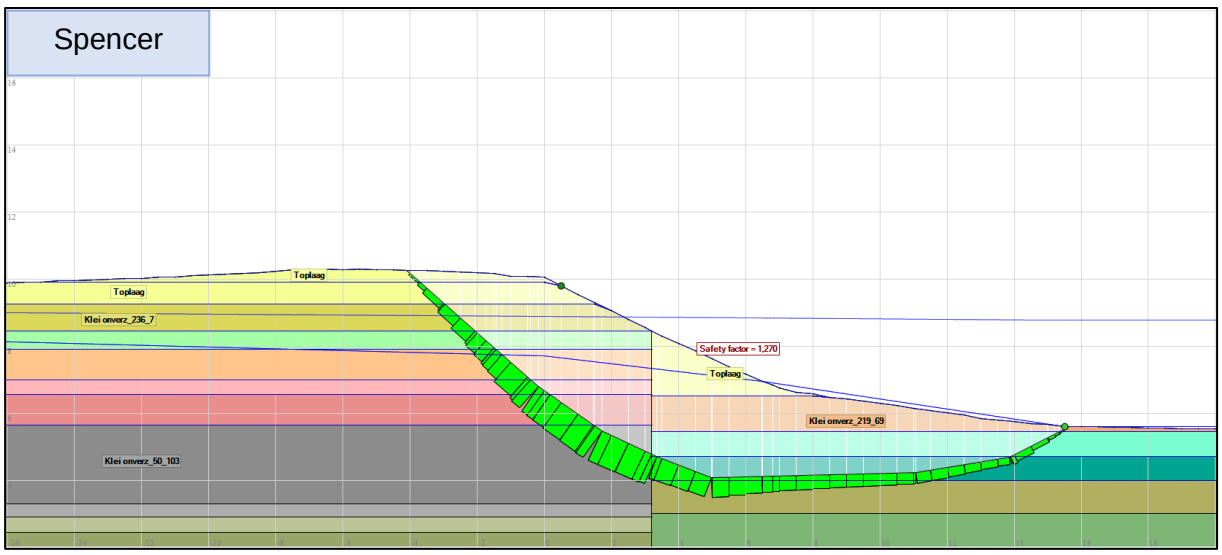

Figures 3.2a-c: The normative sliding surfaces for dike section 6a, as an example, calculated for each of the three selected sliding surface shape model, i.e. respectively Bishop, UpliftVan, and Spencer.

3.3 Probabilistic analysis

The primary objective of this research is not to accurately assess the macro-stability of the WAM river dike, but rather to analyse the three different soil behaviour models in terms of stability and reliability, based on the geotechnical results achieved for the study case of WAM.

For every dike cross section (16), for every soil behaviour model (3), and for every sliding surface shape model (3), a stability factor (144 in total) is established by means of D-Stability at this point. A statistical analysis will be carried out by virtue of the Probabilistic toolkit, which enables extra insight to this dataset of stability factors by generating a reliability index, β, for each one.

For critical state van Duinen et al. (2016) propose an empirically-based correlation: $Y = 0.15\beta + 0.41$. In order to achieve this for the results of this research, the standard deviations of the before-mentioned geotechnical parameters (i.e. ϕ, c', S, m, γ_{sat}, γ_{unsat}, and the dilatancy), are derived from the sample collection tool, for which a normal probability distribution is assumed (truncated for cohesion, as $c' \geq 0$). Furthermore dilatancy and ϕ are assumed to behave 1:1 and $\gamma_{sat} \geq \gamma_{unsat}$. By means of numerical integration the Probabilistic toolkit manages to calculate the reliability index based on an indefinite amount of LEM model runs, for which it performs free variations on the input data (over its complete statistical range), where the probability of failure is based on the uncertainty that comes with every considered soil parameter. The toolkit is also able to present the influence of variations on the probability of failure separately for each stochastic parameter.

Although the macro-stability is dependent on an abundance of parameters, only a maximum of seven are included for the probabilistic analysis for this research: uncertainty in the schematisation of the subsoil, the water level, and the pore pressure, which are directly adopted from Kwakman (2019), are disregarded. This choice has been made in order to avoid side effects in other parameters irrelevant to the soil strength, but also because of a lack of available (statistical) data.

4 Results

4.1 Sample collection tool output: geotechnical parameters

Six different types of soil have been distinguished for the study case of WAM by means of ground drillings and CPTs. Through the available laboratory test results, and the sample collection tool, a set of geotechnical parameters has been established per soil type for all three soil behaviour models (Tab. 4.1a-d), which will serve as input for D-Stability and the probabilistic toolkit, and are discussed in section 5.1.

Table 4.1a: Mohr-Coulomb soil behaviour model geotechnical parameters and the concomitant standard deviation in square brackets.

Soil type	$\gamma_{(un)sat}$ (kN/m^3)	ϕ (°)	c' (kN/m^2)	S (-)	m (-)
Top layer	19.5 [0.8]	31.4 [0.6]	5.24 [1.12]	-	-
Clay (heavy unsat.)	19.5 [0.8]	31.4 [0.6]	5.24 [1.12]	-	-
Clay (heavy)	18.5 [1.2]	34.2 [0.3]	3.06 [0.49]	-	-
Clay (light)	16.6 [1.5]	31.6 [0.8]	4.94 [0.92]	-	-
Peat bog	11.0 [0.6]	31.1 [1.4]	2.11 [1.08]	-	-

Table 4.1b: Peak strength soil behaviour model geotechnical parameters and the concomitant standard deviation in square brackets (light grey values are not considered for this research).

Soil type	$\gamma_{(un)sat}$ (kN/m^3)	ϕ (°)	c' (kN/m^2)	S (-)	m (-)
Top layer	19.5 [0.8]	29.8 [0.3]	7.40 [3.78]	-	-
Clay (heavy unsat.)	19.5 [0.8]	29.8 [0.3]	7.40 [3.78]	0.38 [0.02]	0.93 [0.02]
Clay (heavy)	18.5 [1.2]	25.0 [0.4]	14.63 [3.89]	0.38 [0.03]	0.91 [0.02]
Clay (light)	16.6 [1.5]	26.9 [0.1]	10.10 [3.83]	0.36 [0.02]	0.84 [0.02]
Peat bog	11.0 [0.6]	25.8 [0.1]	6.23 [1.19]	0.38 [0.03]	0.80 [0.02]

Table 4.1c: Critical state soil behaviour model geotechnical parameters and the concomitant standard deviation in square brackets (light grey values are not considered for this research).

Soil type	$\gamma_{(un)sat}$ (kN/m^3)	ϕ (°)	c' (kN/m^2)	S (-)	m (-)
Top layer	19.5 [0.8]	32.6 [0.8]	-	-	-
Clay (heavy unsat.)	19.5 [0.8]	32.6 [0.8]	-	0.35 [0.03]	0.93 [0.02]
Clay (heavy)	18.5 [1.2]	35.0 [1.9]	-	0.32 [0.03]	0.91 [0.02]
Clay (light)	16.6 [1.5]	35.4 [1.7]	-	0.27 [0.02]	0.84 [0.02]
Peat bog	11.0 [0.6]	31.8 [1.4]	-	0.34 [0.02]	0.80 [0.02]

Table 4.1d: Default geotechnical parameters and the concomitant standard deviation in square brackets for sand, which is independent of the soil behaviour model.

Soil type	γ_{sat} (kN/m^3)	γ_{unst} (kN/m^3)	ϕ (°)	c' (kN/m^2)	S (-)	m (-)
Sand	20.0 [0.8]	18.0 [0.8]	30.0 [1.5]	-	-	-

4.2 D-Stability output: stability factors

The LEM model D-Stability is able to give half of the solution to the third research question by presenting a set of stability factors for the three soil behaviour models, and the three sliding surface shape models, calculated for sixteen dike sections that are part of the WAM study case (Tab. 4.2). The total averages and standard deviations for each scenario, as well as the usage of three different sliding surface shape models for each soil behaviour model serve as check of consistency and precision, and are discussed in section 5.2.

Assessing the macro-stability of the WAM dike with the minimum required stability factors as presented in section 2.3 is however not possible. For critical state a different material factor than the one presented by Kwakman (2019) should be considered, as this research employs the *expected* shear strength soil parameters instead of the *characteristic* ones. For Mohr-Coulomb and peak strength, besides a different material factor, also a different damage factor should be implemented, due to the alternative assumptions that come with these soil behaviour models.

Furthermore, without a probabilistic aspect the stability factors for the different soil behaviour models cannot be compared meaningfully: a relatively higher stability factor for Mohr-Coulomb, does not necessarily mean it can be justly considered as more stable, as the uncertainty is yet unidentified.

Table 4.2: Stability factors (*Y*) calculated by D-Stability for all three soil behaviour models, and for all three sliding surface shape models, for the sixteen considered dike sections of WAM.

	Mohr-Coulomb			Peak strength			Critical state		
Dike section (#)	**Bishop *Y* (-)**	**UpliftVan *Y* (-)**	**Spencer *Y* (-)**	**Bishop *Y* (-)**	**UpliftVan *Y* (-)**	**Spencer *Y* (-)**	**Bishop *Y* (-)**	**UpliftVan *Y* (-)**	**Spencer *Y* (-)**
2	2.17	2.25	2.23	1.81	1.78	1.85	1.36	1.37	1.43
2a	1.62	1.62	1.63	1.33	1.33	1.34	1.07	1.07	1.04
3	2.14	2.05	2.07	1.63	1.65	1.65	1.33	1.28	1.33
4	2.38	2.39	2.40	1.74	1.72	1.76	1.30	1.28	1.29
5	1.37	1.33	1.30	1.29	1.23	1.31	1.07	1.01	1.07
6	2.18	2.17	2.21	1.73	1.67	1.70	1.19	1.17	1.21
6a	1.99	1.82	1.88	1.46	1.47	1.54	1.29	1.28	1.27
7	2.32	2.32	2.33	1.93	1.83	1.92	1.44	1.44	1.47
8	2.12	2.07	2.11	1.86	1.83	1.92	1.46	1.45	1.48
9	1.78	1.88	1.86	1.55	1.49	1.57	1.34	1.27	1.30
10	1.98	1.96	1.95	1.89	1.82	1.91	1.60	1.48	1.53
10a	1.05	1.01	1.00	1.27	1.22	1.15	1.12	1.06	1.01
12	1.61	1.58	1.60	1.48	1.49	1.50	1.27	1.32	1.31
14	2.30	2.04	2.25	2.05	1.86	1.99	1.45	1.46	1.51
15	2.41	2.36	2.39	2.13	2.08	2.14	1.66	1.50	1.56
17	2.07	1.88	2.04	1.87	1.65	1.69	1.55	1.37	1.43
Average	1.97	1.92	1.95	1.69	1.63	1.68	1.34	1.30	1.33
Std. dev.	0.39	0.38	0.40	0.27	0.24	0.27	0.18	0.16	0.18

4.3 Probabilistic toolkit output: reliability factors and sensitivity analysis

The second half of the solution to the third research question is achieved through the probabilistic toolkit: the reliability index, β, is calculated for the entire dataset of stability factors for WAM, which is based on the probability distribution of every considered stochastic parameter (complete dataset in Appendix D). The relation between this index and the stability factor is presented in Figures 4.1a-d, including confidence bands, which define the 5% upper and lower limit. All results presented in this section are extensively discussed in section 5.2.

In response to the default equation for the relation between the stability factor and the reliability index presented by van Duinen et al. (2016), the linear trendlines and the concomitant equation and coefficient of determination, R^2, are resolved for every combination of the three sliding surface shape models and the three soil behaviour models as well, which are presented in Table 4.3.

Table 4.3: The equations of the trendlines (in the form $Y = a * \beta + b$) defining the relation between the stability factor and the reliability index, for each soil behaviour model and each sliding surface shape model, complemented by the coefficient of determination, R^2.

	Mohr-Coulomb		Peak strength		Critical state	
Sliding surface shape model	**Equation trendline Y =**	**R^2 (-)**	**Equation trendline Y =**	**R^2 (-)**	**Equation trendline Y =**	**R^2 (-)**
Bishop	0.075β + 1.032	0.776	0.063β + 1.138	0.599	0.058β + 1.027	0.823
UpliftVan	0.073β + 1.045	0.793	0.062β + 1.112	0.574	0.054β + 1.026	0.920
Spencer	0.071β + 1.069	0.836	0.065β + 1.112	0.601	0.057β + 1.020	0.906

The probabilistic toolkit is also able to indicate the influence of each of the stochastic parameters (per soil layer for every considered cross section) for the simulated failure mechanism. For each soil behaviour model, the top 3 influence factors (IFs) are presented in Table 4.4, specified by the percentage of cases a geotechnical parameter is represented.

Table 4.4: The significance of each of the geotechnical parameters considering the macro-stability failure mechanism, defined by the percentage of cases they are part of the three most prominent influence factors (IFs). For Mohr-Coulomb and peak strength, the friction angle, ϕ, also represents the dilatancy, as these parameters react 1:1.

	Mohr-Coulomb				Peak Strength				Critical state			
Geotechnical parameter	**IF 1 (%)**	**IF 2 (%)**	**IF 3 (%)**	**Avg. (%)**	**IF 1 (%)**	**IF 2 (%)**	**IF 3 (%)**	**Avg. (%)**	**IF 1 (%)**	**IF 2 (%)**	**IF 3 (%)**	**Avg. (%)**
ϕ / dilatancy	38	19	10	22	19	13	6	13	13	17	15	15
c'	27	31	35	31	13	4	8	8	-	-	-	-
S	-	-	-	-	60	67	50	59	73	60	54	63
m	-	-	-	-	0	0	0	0	0	0	0	0
γ_{sat}	35	52	54	47	8	15	29	17	15	23	29	22
γ_{unsat}	0	0	0	0	0	2	6	3	0	0	2	1

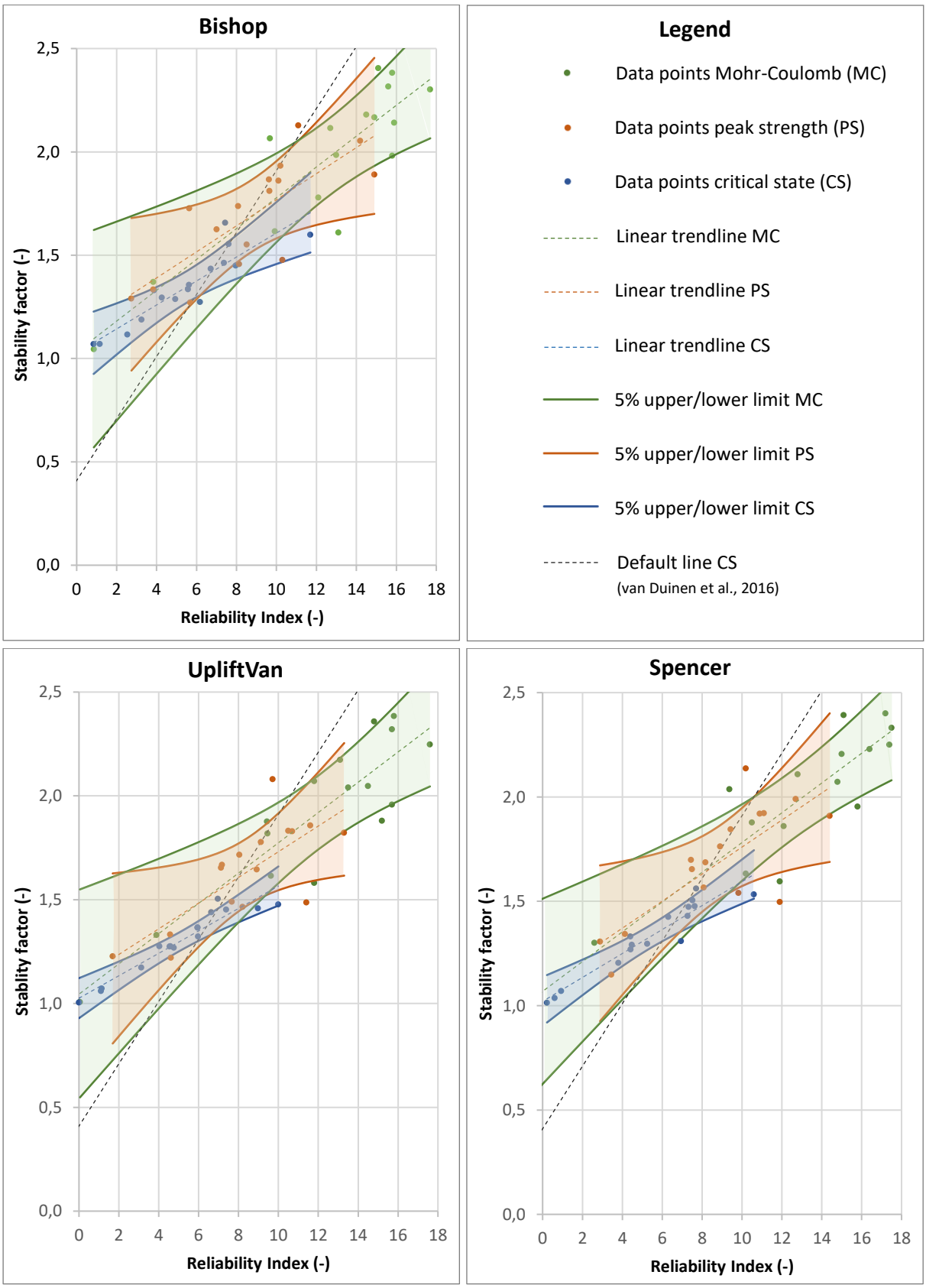

Figures 4.1a-d: The relation between the stability factor, *Y*, and the reliability index, *β*, separately for all three considered sliding surface shape models, presented by the individual data points, a linear trendline and the 5% upper and lower limit, for each soil behaviour model. The black dotted line defines the default relation for critical state proposed by van Duinen et al. (2016).

Figure 4.2 again presents the relation between the stability factor and the reliability index, only all 144 data points of each sliding surface shape model are included in one graph, and more importantly the size of the data point varies to represent additional information: the slope of the concomitant dike section. Only two out of the sixteen considered dike sections consist primarily of sand (instead of clay): the solid black border around eighteen data points outline these.

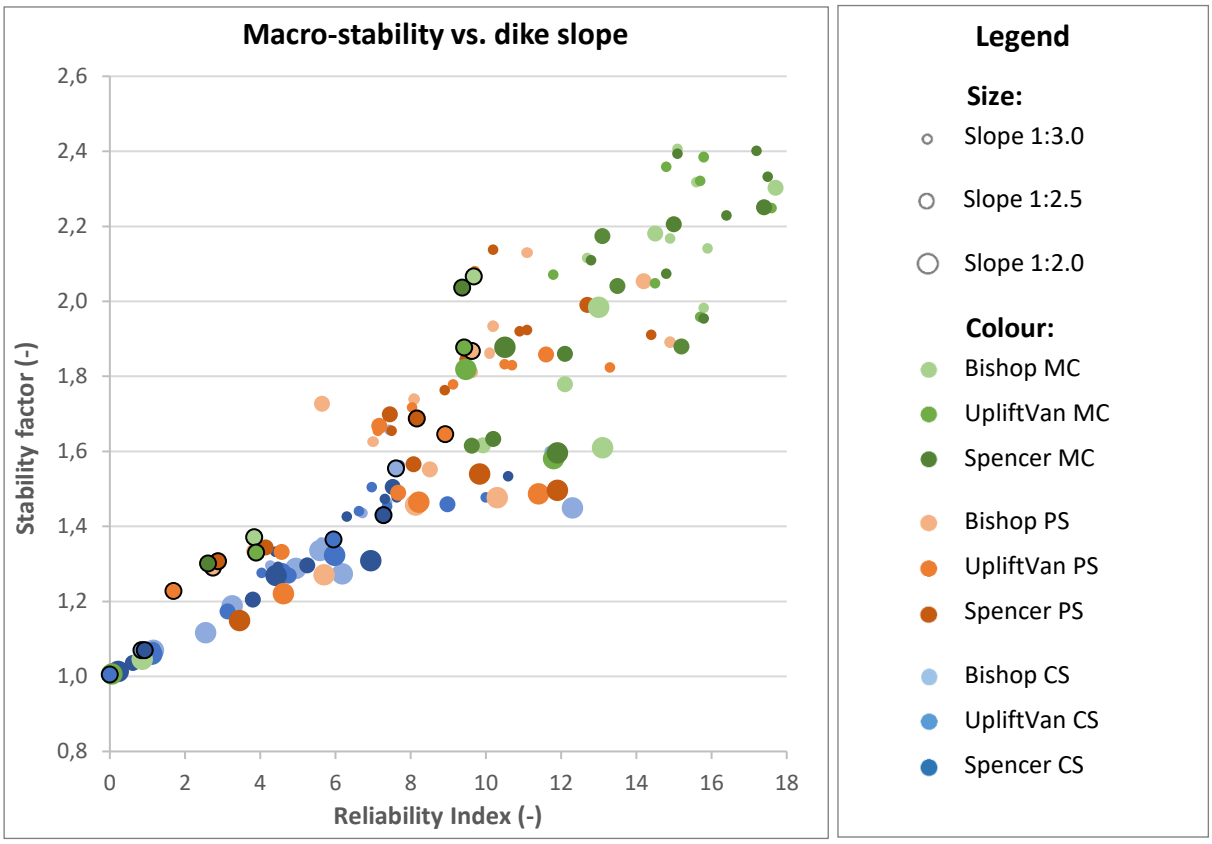

Figure 4.2: The relation between the stability factor, *Y*, and the reliability index, *β*, combined for all three considered sliding surface shape models, presented by the individual data points, where the size of the data point represents the slope of the dike section. A data points with a solid black border illustrates a dike section that mainly consists of sand.

5 Discussion

5.1 Assumptions and data schematisation

Soil behaviour models

In this research three recognised soil behaviour models are assessed considering the inward macro-stability of a river dike, i.e. Mohr-Coulomb, peak strength and critical state. The concomitant geotechnical parameters, their uncertainty and assumptions considering the soil behaviour are not completely unambiguous however.

The three soil behaviour models that can be distinguished based on the assumed amount of axial strain the soil is exposed to during the compression tests: in this research for Mohr-Coulomb 2%, for peak strength the amount of strain is dependent on the maximum soil strength, and for critical state 25%. Besides the fact that the assumed geotechnical parameters are based on a limited sample collection, and therefore only reliable to a certain extent, considering the peak strength it must be argued that the maximum will not occur for the same amount of axial strain for every soil type: i.e. a scenario where the soil strength of every soil type is at its peak can never happen, which is currently not quantitatively accounted for. However the critical state model can also be believed to be a conservative approach, as also not all soil types will reach its ultimate strength at the same amount of axial strain.

For two of the three soil behaviour models, also a distinction between drained and undrained behaviour must be made, which is described to be predominantly influential for the soil strength by Kwakman (2019):

- For Mohr-Coulomb only the drained geotechnical parameters are considered due to the low axial strain: moreover the average shear strength values of this soil behaviour model are less comprehensive and presumably less reliable due to relatively more scatter of the data points, as soil samples with a high effective stress are excluded.
- For critical state, general guide lines are assumed for the drained/undrained soil behaviour: van Duinen et al. (2016) claim that for soil types with a high permeability (i.e. sand) drainage is able to take place during macro-instability, while for soil types with a low permeability (i.e. clay and peat bog) minimal drainage will occur. In regard of the two types of anthropogenic dike material (which have a moderate permeability), for the macro-stability assessment of WAM Kwakman (2019) assumed drained behaviour for the top layer, which is confirmed by van Duinen et al. (2016), as employing undrained soil behaviour would likely overestimate the soil strength. The heavy, unsaturated dike material is expected to behave undrained, provided it is located directly on top of soil layers with a low permeability and rapid sliding of the dike slope. Despite that this would be the case for practically every WAM dike section, due to uncertainty about the behaviour of the anthropogenic clay, and also as a result of

the physically impossible values for the strength increase exponent, *m*, the decision was made to also calculate with the drained soil strength parameters, which is regarded as the most safe approach. In this research however, the latter assumption is not adhered to: as the primary objective of this research is to evaluate the differences in the three soil behaviour models instead of an accurate case-specific macro-stability assessment, undrained soil strength parameters are employed (including a default strength increase exponent).

- The soil behaviour for the peak strength model is disputed, as deformation of the soil will be considerably different for brittle material and resilient/plastic material. As suggested by van Duinen (2015) undrained soil behaviour for the peak strength is probable and acceptable, therefore the same drained/undrained behaviour as for critical state is presumed.

As mentioned in section 2.1, by employing the ultimate strength as the normative soil strength in the LEM models, one automatically presumes the shear strength to be mobilised along the entire sliding surface. Despite the fact that a considerably large amount of deformation at the bottom of the sliding surface is required for full mobilisation, this hypothesis is proven to be fairly plausible for critical state due to the high axial strain associated to this soil behaviour model. This is not the case for Mohr-Coulomb and peak strength. In order to achieve the most realistic macro-stability interpretation for these two soil behaviour models, differences in the mobilised shear strength along the entire sliding surface should be implemented. This could possibly be achieved by the ADP method.

In order to account for anisotropy within the subsoil, the ADP-method is recommended. This stability analysis subdivides the sliding surface into three zones: Active, Direct, and Passive than find their origin in the Rankine theory. In general the soil is assumed to be pressed together in the active zone; in the direct zone the soil grains slide over each other; in the passive zone the soil is pulled apart. The soil behaviour within these three zones is believed to correspond with respectively triaxial compression tests, direct simple shear tests, and triaxial extension tests (CUR, 1992, TAW, 2001; van Duinen, 2014).

On condition of considerable deformation of the soil structure (i.e. critical state), each test and therefore each sliding surface zone is believed to achieve its maximum strength. In case of no to little deformation (i.e. Mohr-Coulomb and peak strength) this will not be realised: given low axial strain, the active zone will be mobilised, while the passive zone will be not, as a consequence of differences in the resilience of the soil. This study has assumed the shear along the entire sliding surface zone to be equivalent and to occur simultaneously, which results in an overestimation of the maximum mobilizable shear strength. It would be recommended to implement different values of the shear strength parameters over the length of the sliding surface: conventional values for the active zone, and practically zero for the passive zone (van Duinen, 2017). For some of the selected WAM dike sections, depending on

the geohydrological situation, the passive zone is already associated to a soil strength of zero. This was employed for areas for which high water was determined to induce seep pressure ("kweldruk") in the sandy subsoil, leading to an uplifting motion of the hinterland, ultimately resulting in the bursting of the cover layer, and loss of soil-integrity (van Duinen et al., 2016). The direct zone is somewhat a grey area. A correlation between the active and direct zone, and the soil behaviour, i.e. respectively soil strength derived from TC tests and DSS tests is proposed, however still very questionable. This matter, plus the fact that the subdivision of the three zones (dependent on the shape of the sliding surface) is very unreliable, makes this vital method arguable at the same time. An alternative solution to account for anisotropy would be employing a numerical model that does not assume a static equilibrium. These models are however known to be considerably sensitive to the initial stresses: assuming both the soil strength and the imposed loads as dynamic, will induce additional uncertainty due to the feedback mechanisms. A static equilibrium, as applied in this research, is presumably more conservative, however associated to much more certainty.

Geotechnical parameters

By means of the soil sample collection tool, geotechnical parameters have been established for each soil behaviour model (Tab. 4.1a-d), which serve as the solution to the first research question: how do these compare? In every macro-stability assessment a separation is made between the saturated and unsaturated volumetric weight, γ, which is naturally regulated by the phreatic level. However for all soil types, except for sand, van Duinen et al. (2016) recommend to make no quantitative distinction, as the soil above the phreatic level still holds a lot of water. The volumetric weight parameters determined for this case are well within range of the default values presented for common soil types by van Duinen et al. (2016). It must be noted that the volumetric weight of the heavy unsaturated clay is higher than the heavy clay due to different origin and content of the soil.

The presented soil strength parameters also seem to be very plausible. Considering drained soil behaviour the critical state model shows the relatively highest values for the angles of friction. However this is the only soil behaviour model for which the soil is remoulded, due to the high axial strain. Therefore it is also the only model without cohesion. For both Mohr-Coulomb and peak strength the drained soil strength consists of the friction angle and cohesion, which are together much stronger than the soil strength parameter presented for critical state. As expected, the standard deviations presented for cohesion are noticeably high: this parameter is not directly derived from the TC or DSS tests, but is a product of extrapolation of the data points towards the y-axis where the effective normal stress is zero. As the regression lines are fitted with least-squares methods for which the uncertainty increases away from the mean, the cohesion becomes highly uncertain, partly for statistical reasons.

5.2 Assessment of dike macro-stability

Stability and reliability

With the geotechnical parameters established by the soil sample collection tool serving as input, the stability factors, Y, and concomitant reliability indices, β, could be determined by respectively D-Stability and the Probabilistic Toolkit, for sixteen selected WAM dike sections (Tab 4.2 and App. D). These results are able to give answer to the third research question: will the implementation of the peak strength, rather than the critical state, result in a different dike design, will it lead to more stability, and is it equally reliable under fixed stress conditions?

The stability factors are calculated for each soil behaviour model, but also for each sliding surface shape model, resulting in 144 values. The averages presented for each scenario display a clear relation. Comparing the three soil behaviour models it is evident that the critical state produces the lowest stability factors, which can be explained by the conservative soil strength assumptions, followed by the peak strength, which assumes the same drained/undrained soil behaviour, but less conservative soil strength assumptions, where Mohr-Coulomb demonstrates the highest stability factors, which can be associated to the non-conservative soil strength premise and the exclusively drained soil behaviour. Looking within the soil behaviour models, at the sliding surface shape models, small-scale differences, yet an apparent correlation can be distinguished: on average Bishop presents the highest stability factors, followed by Spencer, where UpliftVan produces the lowest stability factors. This tendency can be accounted for by the shape restrictions and is verified by the standard model factors, Y_d, presented in section 2.2. The standard deviations, also presented in Table 4.2, is the first indication that critical state is considerably less variable than the other two soil behaviour models, and hence it could be relied upon with more confidence.

In order to give more value to these factors, and to address the last part of the third research question, a reliability index is determined for each stability factor, which is based on the uncertainty (extracted from the soil sample collection tool) of seven parameters that serve as input for the LEM model. Table 4.3 presents the relationship between the stability factor and the reliability index quantitatively for each scenario, in the form of an equation of the trendline of the data points ($Y = a \cdot \beta + b$), complemented by the coefficient of determination, R^2. The starting number, b, which is the Y for $\beta = 0$, is evidently the highest for peak strength, while the slope or gradient of the line, a, is the highest for Mohr-Coulomb. Considering the determination coefficient, critical state is clearly the soil behaviour model that shows the least variance in the dependent variable (i.e. smallest amount of data point scatter). Figures 4.1a-d display these relationships graphically, separately for each sliding surface shape model. It can be observed that areas around the best fit of the data points for each soil behaviour model are largely comparable, and therefore barely distinctive. The default line for critical state established by van Duinen et al. (2016) however, can be associated to a considerably lower starting number (not even half), and a much higher gradient of the line (at least double), in comparison to the

ones proposed by this research. This means that the stability-reliability equations proposed by this research, no matter what soil behaviour model, produce a higher reliability index than the standard equation for the same stability factor. This anomaly is presumably the result of the limited amount of stochastic parameters employed in this study using the probabilistic toolkit, which naturally creates less uncertainty. One could consider to implement uncertainty regarding for instance: the sliding surface circle, geometry, hydraulic pressure, POP, and/or consolidation.

Uncertainty

Figures 4.1a-d are also able to give extra insight through the 5% upper/lower limit lines for each soil behaviour model, producing confidence bands based on the variance of the data points in respect to the linear trendline. As expected, these are similar to a great extent when comparing the sliding surface shape models. It can be observed that the uncertainty for critical state is quite modest (narrow confidence bands), where peak strength is unable to convince for a relatively low or high reliability. Mohr-Coulomb consists of particularly an abundance of data points with a high stability factor and a high reliability index, and therefore falls short to persuade for lower values.

As mentioned in section 2.3 the minimum required stability factor, Y_{min}, when calculating with the *characteristic* geotechnical parameters of the critical state soil behaviour model and employing the Bishop, UpliftVan and Spencer shape model are respectively 1.43, 1.36 and 1.38. For this research however, the *expected* geotechnical parameters are employed, which have to be associated to a higher required stability factor: CUR (2006) proposes a critical stability threshold of Y_{min} = 1.6 (depending on the standard model factor, Y_d, and the material factor, Y_m). For this value, which is critical for the assessment of dike macro-stability, the deterministic reliability indices (following from the trendline equations for Y = 1.6), and the confidence bands that originate from Figures 4.1a-d, are presented in Table 5.1. It can be observed that for Mohr-Coulomb and peak strength relatively comparable deterministic reliability indices are presented, around 7.5 - 7.6, despite the existent differences in the normative equations introduced in Table 4.3. In contrast, critical state is able to present a deterministic reliability index of at least 9.9. For the crucial stability factor of 1.6, the peak strength presents the widest confidence bands, stretching from below zero, to a maximum of

Table 5.1: The deterministic reliability index, β, and the concomitant confidence range (in some cases interpolated) for Y = 1.6, for each soil behaviour model and each sliding surface shape model.

	Mohr-Coulomb		Peak strength		Critical state	
Sliding surface shape model	**Deterministic β**	**Confid. range β**	**Deterministic β**	**Confid. range β**	**Deterministic β**	**Confid. range β**
Bishop	7.6	0.8 - 10.4	7.3	<0 - 10.5	9.9	8.0 - 14.4
UpliftVan	7.6	1.4 - 10.2	7.9	<0 - 12.3	10.6	9.1 - 13.2
Spencer	7.5	2.2 - 10.0	7.5	<0 - 10.7	10.2	8.6 - 12.7

12.3. Mohr-Coulomb falls within the same spectrum, however with a minimum above zero. Critical state manages to produce both a much higher, as a much more narrow and precise uncertainty range. The differences per sliding surface shape model, within each soil behaviour model, are negligible, and therefore only verify the results in general.

Influence

The separate influence of each geotechnical parameter on the calculated reliability indices, which directs the second research question, is presented in Table 4.4 per soil behaviour model. For Mohr-Coulomb only five out of the seven selected parameters are considered, due to the assumed drained soil behaviour. The friction angle, dilatancy (together 22%) and, in a greater extent, cohesion (31%) have a decent impact on the reliability index. This relation was to be expected, especially due to the relatively large standard deviation for the cohesion. Surprisingly, the saturated volumetric weight is the factor with the greatest influence (47%), which is mainly the case for dike sections with a fair amount of stratification and a sliding surface composed of dike material exclusively. As anticipated, for both peak strength and critical state the influence of the shear strength ratio is superior (respectively 59% and 63%). It must be noted that the influence of cohesion is considerably smaller for peak strength (8%) than for Mohr-Coulomb. This can be clarified by the relatively small amount of soil layers for which drained behaviour is assumed. Naturally cohesion is not included for critical state due to the fully remoulded soil behaviour. It can be confirmed that the assumptions considering drained/undrained soil behaviour, are undeniably decisive, however also hard to substantiate.

The last research question concerns the influence of alternative factors on dike stability. Figure 4.2 presents two other factors that could potentially influence the relationship between the stability factor and reliability index, i.e. the dike slope and the dominant dike material. As expected, the larger data points that represent dike sections with a relatively steep slope, can be associated to a generally lower stability factor, and therefore are less stable. A correlation with the reliability index is not distinguishable based on these results. With regard to the primary soil type, no more than two out of sixteen dike sections consist mostly of sand. These can be associated to a relatively low stability factor (within their own soil behaviour model), and also a low reliability index. Particularly the small differences between the soil behaviour model are of interest. These results can be clarified by the relatively high phreatic level and the geotechnical parameters assumed for sand: only drained behaviour, a relatively small angle of friction, and lack of cohesion.

6 Conclusion

In this research three soil behaviour models have been distinguished: Mohr-Coulomb, which used to be normative for dike macro-stability assessment until a few years ago, peak strength, and critical state, which has been the standard since the implementation of WBI 2017. Although the latter is currently nationally favoured over the first, due to the distinction between drained and undrained behaviour, Mohr-Coulomb is still included in this research, serving as validation and point of reference.

The primary objective of this study was to figure out whether using the peak strength soil behaviour model is preferred over the critical state, considering the stability and reliability. This is of great significance as the latter approach is collectively considered as too conservative, i.e. the strength of a dike is currently underestimated, while the peak strength is still relatively uncharted in this context.

For sixteen dike sections of the WAM case study, for the three mentioned soil behaviour models, and for three selected sliding surface shape models (i.e. Bishop, UpliftVan and Spencer), stability calculations have been executed by means of the LEM model D-Stability, followed by reliability calculations in the Probabilistic toolkit. From the results it can be established that both Mohr-Coulomb and peak strength produce considerably higher stability factors than critical state, which was to be expected due to the differences in soil strength. However the first two can also be associated to a relatively lower reliability, plus much more uncertainty.

The influence of a specific soil behaviour model and its implicit assumptions on the macro-stability assessment is indisputable. This research has demonstrated that for Mohr-Coulomb the reliability is primarily controlled by the saturated volumetric weight, and the drained soil strength parameters (including cohesion), while the other two are particularly dependent on the shear strength ratio. If more input parameters would be considered as stochastic, presumably alternative correlations would have showed up. Factors such as the dike slope and the predominant soil type have proven to be significant, regardless of the soil behaviour model.

It can be concluded that comparing the three soil behaviour models, critical state, although undervaluing the strength of a dike, is able to assess the macro-stability the most precise, and also produces the highest reliability. Based on the WAM case study, which must be specified as limited due to the short quantity of soil samples and the restricted heterogeneity of the geometry, lithology, and geotechnical parameters, it is suggested to maintain the ultimate strength of a soil type as normative in case of dike macro-stability assessment: the implementation of peak strength does result in a more stability, but is far from able to present the same degree of reliability as critical state. Whether the results presented in this research,

and this conclusion will be similar for other dikes, possibly in other environments, is currently unresolved. It is therefore recommended to perform a similar case study for smaller dikes along local river and/or canals. Integration with results from this study would probably lead to less uncertainty in the lower ($\beta < 6.0$) and higher ($\beta > 10.0$) bandwidth of reliability.

References

Bakker, H., Breedeveld, J., & Teunissen, H. (2011). Analyse Macrostabiliteit Dijken met de Eindige Elementen Methode, Deltares, Rijkswaterstaat – Ministerie van Infrastructuur en Milieu, 1-50.

Bishop, A.W. (1955). The use of the slip circle in the stability analysis of slopes, Geotechnique 5(1), 7-17.

Coulomb, C.A. (1776). Essai sur une application des règles de maximis et minimis a quelques problèmes de statique, relatifs a l'architecture, Mémoires de Mathématique de l'Académie Royale des Sciences, Paris, 7, 343-382.

Crabb, G.I., & Atkinson, J.H. (1991). Determination of soil strength parameters for the analysis of highway slope failures, In Slope stability engineering: developments and applications (ed. R. Chandler), London: Thomas Telford, 13-18.

CUR (1992). Construeren met grond – Grondconstructies op en in weinig draagkrachtige en sterk samendrukbare ondergrond, 162, Civieltechnisch Centrum Uitvoering Research en Regelgeving, 1-564.

CUR (2006). Oeverstabiliteit bij zandwinputten – deel A aanbevelingen, 130, versie 5.9, Civieltechnisch Centrum Uitvoering Research en Regelgeving, 1-22.

de Bruijn, K., & van der Doef (2011). Gevolgen van overstromingen – Informatie ten behoeve van het project Waterveiligheid in de 21e eeuw, Deltares, 1-78.

de Waal, J.P. (2016) Basisrapport WBI 2017, Versie 1.1, Deltares, 5-73.

Deltares (2016). D-Foundations – CPT based foundation engineering – User manual, Deltares, version 16.1, 1-282.

Deltares (2017). D-Geo Stability – Slope stability software for soft soil engineering – User manual, version 18.1, 1-288.

Hegnauer, M., Beersma, J.J., van den Boogaard, H.F.P., Buishand, T.A., & Passchier, R.H. (2014). Generator of Rainfall and Discharge Extrems (GRADE) for the Rhine and Meuse basins – Final report of GRADE 2.0, Deltares, 1-84.

Hertogh, K.K., & Stellema, G.A.M. (2018). Grondonderzoek Sterke Lekdijk Wijk bij Duurstede / Amerongen (WAM) – Resultaten terrein- en laboratoriumonderzoek, Wiertsema-Inpijn-Blokpoel V.O.F., 1-18.

Huizinga, F. (2012). The economics of flood prevention: A Dutch perspective, CPB Netherlands Bureau for Economic Policy Analysis, 2-5.

Janssen, W. (2018). Geotechnisch onderzoek Ravenstein-Lith proevenverzameling met D70, S, M en POP alsmede Phi, Arcadis, Waterschap Aa en Maas, 46.

Kwakman, L. (2019). Rapport: Beoordeling binnen- en buitenwaarts macrostabiliteit - Dijkversterking Wijk bij Duurstede – Amerongen, Sweco & Arcadis, 1-64.

Larsson, R. (1980). Undrained shear strength in stability calculation of embankments and foundations on soft clays, Canadian Geotech, J., 17(4), 591-602.

NEN (1992). Geotechniek – Bepaling van schuifweerstands- en vervormingsparameters van grond Triaxiaalproef, NEN 5117, Nederlands Normalisatie-instituut, 1-26.

Pieterse, N., Knoop, J., Nabielek, K., Pols, L., & Tennekes, J. (2009). Overstromingsrisicozonering in Nederland, Planbureau voor de Leefomgeving, 9-18.

RCE (2013). Een toekomst voor dijken: handreiking voor de omgang met dijken als cultureel Erfgoed, Cultural Heritage Agency of the Netherlands, 7-26.

Řeřicha, P. (2004). Mohr-Coulomb Failure Condition and the Direct Shear Test Revisited, Acta Polytechnica, Vol. 44, No. 5-6, 93-96.

Schofield, A.N. (2006). Disturbed Soil Properties and Geotechnical Design, Thomas Telford, 1-160.

Schofield, A.N., & Wroth, P. (1968). Critical State Soil Mechanics, McGraw-Hill, 1-218.

Slomp, R. (2012). Flood Risk and Water Management in the Netherlands, Rijkswaterstaat Ministry of Infrastructure and the Environment, 11-34.

Spencer, E. (1967). A Method of Analysis of the Stability of Embankments Assuming Parallel Inter-Slice Forces, Geotechnique, 17, 11-26.

Sweco & Arcadis (2018). Rapport Kader Ruimtelijke Kwaliteit Dijkversterking Wijk Bij Duurstede – Amerongen, Hoogheemraadschap De Stichtse Rijnlanden, 3-59.

TAW (2001). Technisch Rapport Waterkerende Grondconstructies – Geotechnische aspecten van dijken, dammen en boezemkaden, Technische Adviescommissie voor de Waterkeringen, 1-300.

Terzaghi, K., Peck, R.B., & Mesri, G. (1996). Soil Mechanics in Engineering Practice, Third Editionm, John Wiley & Sons, Inc. New York, 241-289.

Van, M.A. (2001). New approach for uplift induced slope failure, Proc., 15th International Conf. Soil Mechanics Geotechnology Engineering, Vol. 3, 2285-2288.

Van der Meij, R. (2012). Afschuiving langs een vrij glijvlak. Geotechniek, nr.1, 34-37.

van der Veen, C., Horvat, E., & van Kooperen, C.H. (1981). Grondmechanica met beginselen van de funderingstechniek, Waltman, 53-229.

van Duinen, T.A. (2010). SBW Werkelijke sterkte van dijken - validatie WS15: Synthese resultaten stabiliteitsanalyses onderzoekslocaties, Deltares, Versie 1.

van Duinen, T.A. (2013). Back analyses of dikes that withstand a high water level, Deltares, Memo, 1-20.

Van Duinen, T.A. (2014). Handreiking voor het bepalen van schuifsterkte parameters – WTI 2017 Toetsregels Stabiliteit, Deltaters, 1-98.

van Duinen, T.A. (2015). Toepassen van de piekwaarde van de ongedraineerde schuifsterkte - WTI 2017 Toetsregels Stabiliteit, Deltares, 1-23.

van Duinen, T.A. (2016). Memo – Default waarden voor Pre Overburden Pressure (POP) voor macrostabiliteit, Deltares, 1-7.

van Duinen, T.A., van Deen, J.K., & de Bruijn, H. (2016). Schematiseringshandleiding macrostabiliteit, Rijkswaterstaat Ministry of Infrastructure and the Environment, 9-173.

Verruijt, A. (2001). Grondmechanica, Technische Universiteit Delft, 6-290.

Visser, H., Muijs, J.A., Heijnen, W.J., Mazure, P.C., van Ooijen, D.C., Pachen, H.M.A., Termaat, R.J., Vermeer, P.A. & Vrouwenvelder, A.W.C.M. (1988). Leidraad cel- en Triaxiaalproeven, Technische Adviescommissie voor de Waterkeringen, Rijkswaterstaat, Hydraulic Engineering Reports, 12-61.

Zwanenburg, C., van Duinen, A., & Rozing, A. (2013). Technisch Rapport Macrostabiliteit, Deltares, 7-13.

Zwanenburg, C. (2016) Blauwdruk Eindige Elementen Methode: POV-Macrostabiliteit, Deltares, 1-18.

Appendices

Appendix A: Ground drilling result – DP47+006 (hinterland)

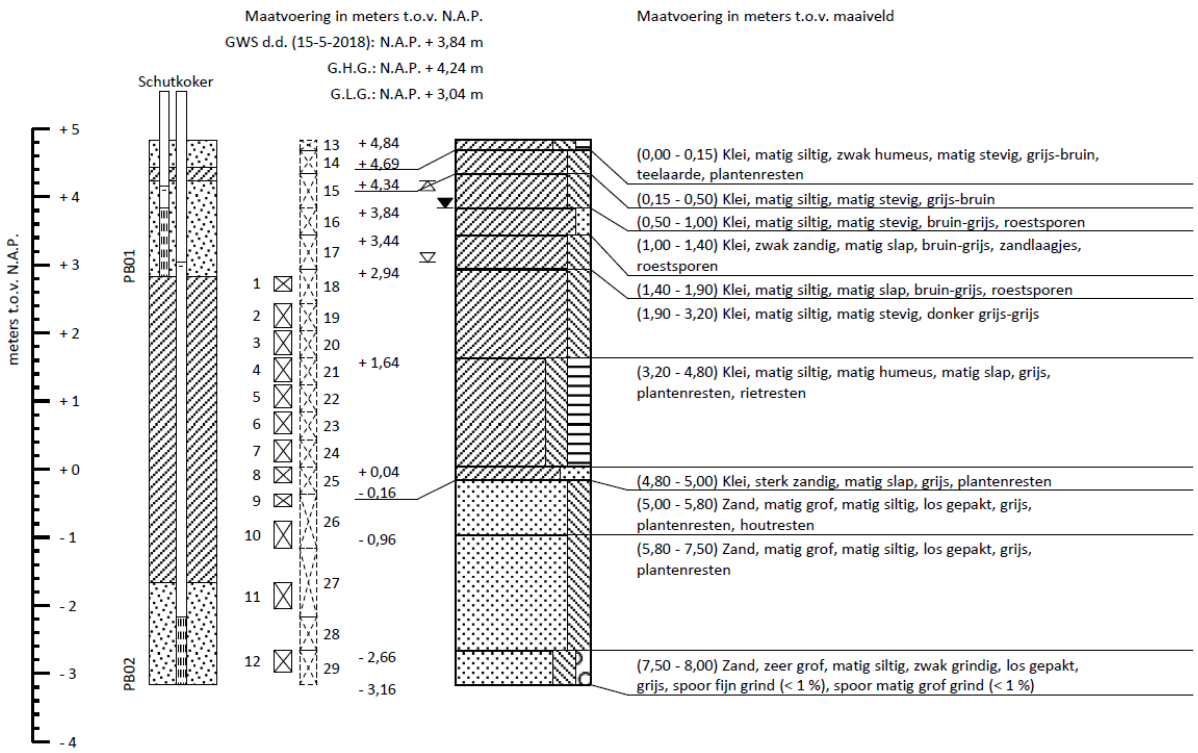

Appendix B: Cone penetration test result – DP49+019 (hinterland)

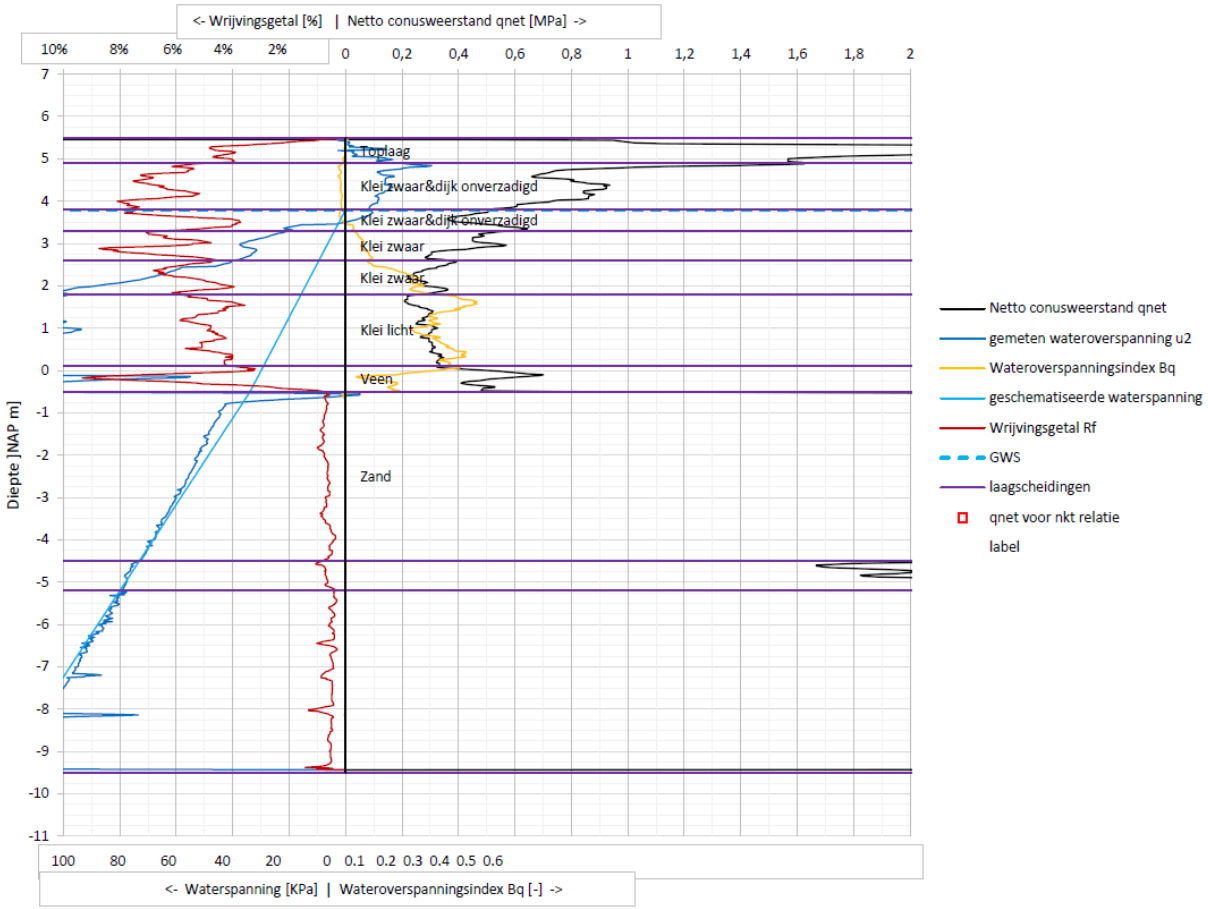

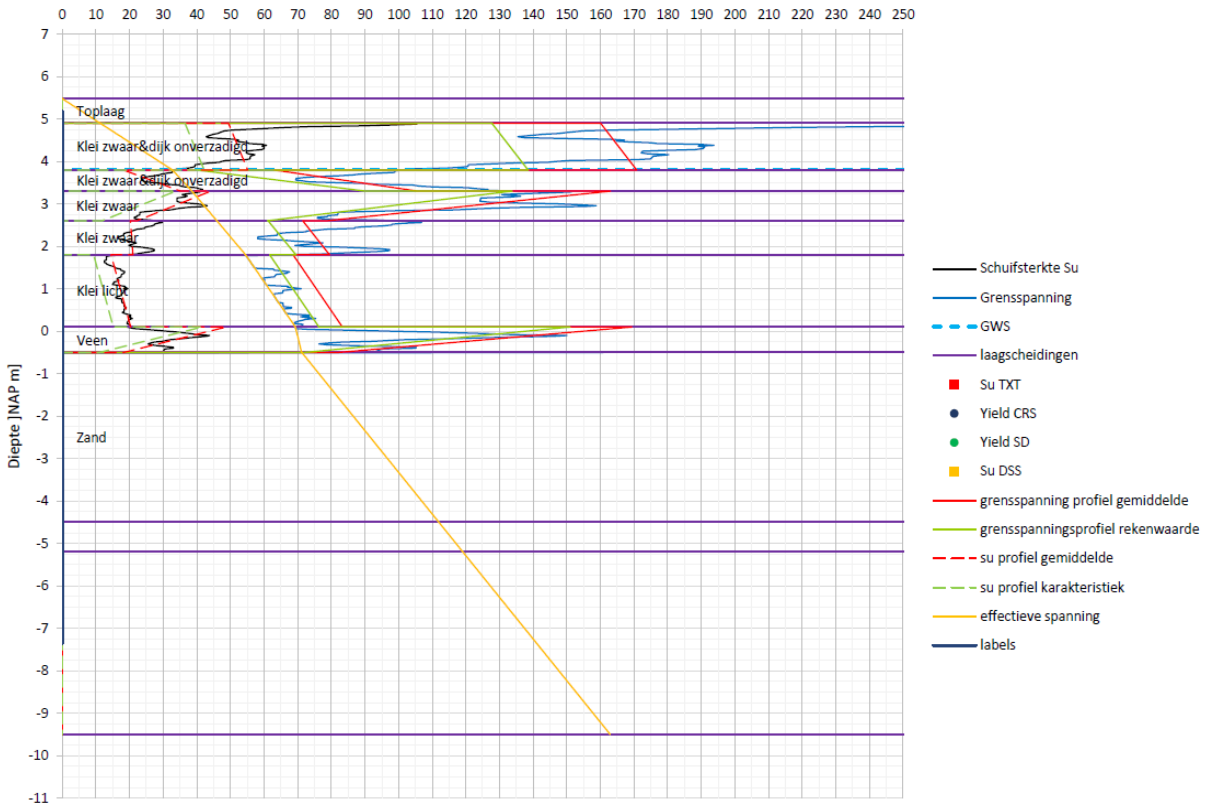

Appendix C: Triaxial compression test results – DP47+006 (hinterland)

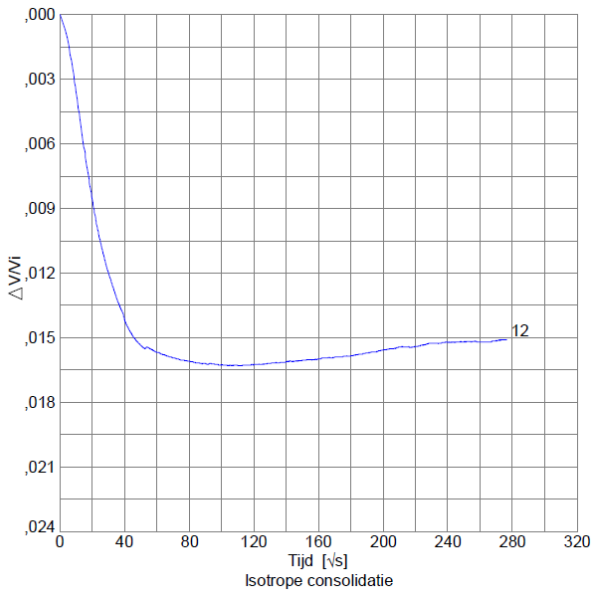

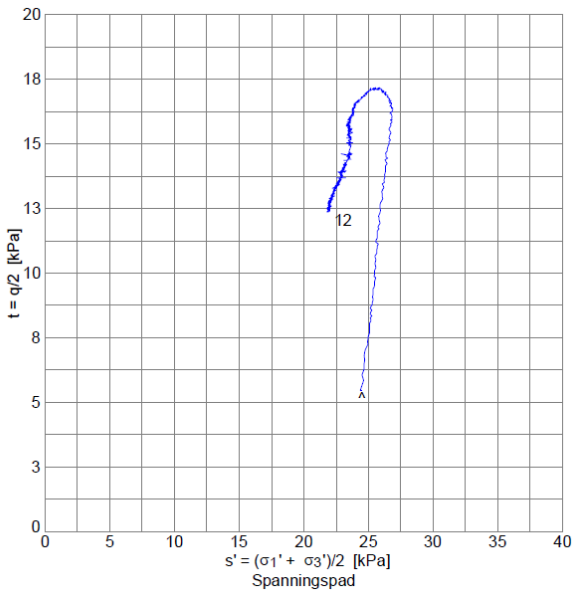

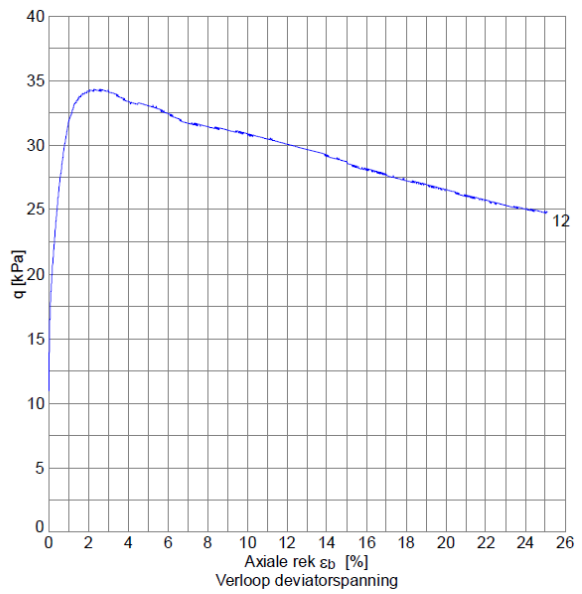

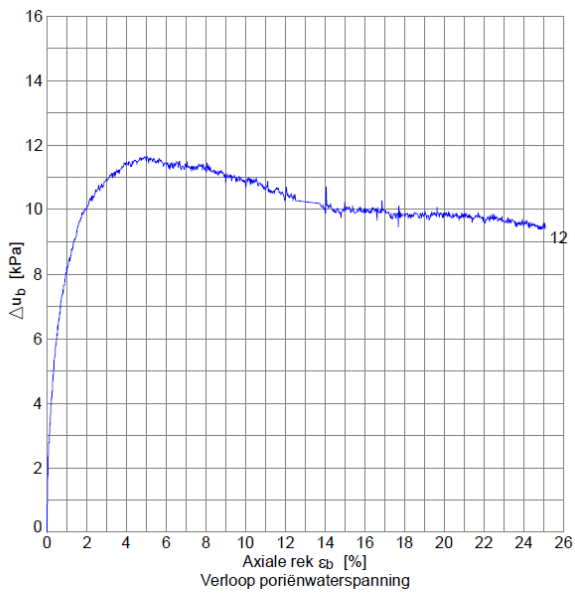

Proefstuk		D_i mm	h_i mm	ρ_i kg/m^3	ρ_{dr} kg/m^3	w_i %	w_e %	σ_c' kPa	u_{bk} kPa	B-waarde	S_u kPa	$\varepsilon_{b;50}$ %	$E_{undr;50}$ MPa	stop-criterium
———	12	50,1	99,7	1548	897	72,5	72,3	19	300	0,97	17,2	0,28	4,20	ε_b = 25 %

Boringnummer : DP47+006_B_AL
Monsternummer : M002-a1
Diepte t.o.v. N.A.P. : 2,32 m
Grondsoort : Klei, zwak siltig, zwak humeus, plantenresten

Monsterklasse : 1
Type proef : K0 consolidatie, ongeroerd
Uitvoeringsprocedure : eentraps
Beproevingssnelheid : 12: 0,016 %/h
K0-waarde : 12: 0,63

Appendix D: Complete macro-stability results dike sections

MC	Bishop			UpliftVan			Spencer		
Dike section (#)	Stab. factor (-)	Reliability Index (-)	$P_{failure}$ (%)	Stab. factor (-)	Reliability Index (-)	$P_{failure}$ (%)	Stab. factor (-)	Reliability Index (-)	$P_{failure}$ (%)
2	2.167	14.90	0.00	2.248	17.60	0.00	2.229	16.4	0.00
2a	1.616	9.92	0.00	1.615	9.63	0.00	1.633	10.20	0.00
3	2.141	15.90	0.00	2.048	14.50	0.00	2.073	14.8	0.00
4	2.383	15.80	0.00	2.385	15.80	0.00	2.401	17.2	0.00
5	1.371	3.84	0.01	1.330	3.89	0.01	1.301	2.61	0.45
6	2.181	14.50	0.00	2.174	13.10	0.00	2.206	15.00	0.00
6a	1.985	13.00	0.00	1.819	9.46	0.00	1.878	10.5	0.00
7	2.317	15.60	0.00	2.321	15.70	0.00	2.332	17.5	0.00
8	2.115	12.70	0.00	2.071	11.80	0.00	2.109	12.8	0.00
9	1.779	12.10	0.00	1.880	15.20	0.00	1.860	12.1	0.00
10	1.982	15.80	0.00	1.958	15.70	0.00	1.954	15.80	0.00
10a	1.046	0.86	19.50	1.007	0.05	47.90	0.998	-0.18	57.10
12	1.610	13.10	0.00	1.581	11.80	0.00	1.596	11.90	0.00
14	2.303	17.70	0.00	2.041	13.50	0.00	2.251	17.40	0.00
15	2.406	15.10	0.00	2.358	14.80	0.00	2.393	15.10	0.00
17	2.066	9.68	0.00	1.877	9.43	0.00	2.037	9.37	0.00
Avg.	1.967	12.53	1.22	1.920	12.00	2.99	1.953	12.41	3.60

PS	Bishop			UpliftVan			Spencer		
Dike section (#)	Stab. factor (-)	Reliability Index (-)	$P_{failure}$ (%)	Stab. factor (-)	Reliability Index (-)	$P_{failure}$ (%)	Stab. factor (-)	Reliability Index (-)	$P_{failure}$ (%)
2	1.811	9.65	0.00	1.778	9.13	0.00	1.845	9.44	0.00
2a	1.334	3.84	0.01	1.332	4.57	0.00	1.344	4.14	0.00
3	1.625	7.01	0.00	1.654	7.13	0.00	1.654	7.50	0.00
4	1.738	8.09	0.00	1.717	8.04	0.00	1.763	8.91	0.00
5	1.290	2.74	0.31	1.228	1.69	4.56	1.307	2.88	0.20
6	1.727	5.64	0.00	1.668	7.17	0.00	1.699	7.45	0.00
6a	1.457	8.13	0.00	1.465	8.21	0.00	1.540	9.83	0.00
7	1.933	10.20	0.00	1.829	10.70	0.00	1.923	11.10	0.00
8	1.861	10.10	0.00	1.832	10.50	0.00	1.920	10.90	0.00
9	1.552	8.51	0.00	1.490	7.67	0.00	1.566	8.08	0.00
10	1.891	14.90	0.00	1.823	13.30	0.00	1.910	14.40	0.00
10a	1.271	5.69	0.00	1.221	4.61	0.00	1.149	3.45	0.03
12	1.477	10.30	0.00	1.487	11.40	0.00	1.497	11.90	0.00
14	2.054	14.20	0.00	1.858	11.60	0.00	1.991	12.70	0.00
15	2.129	11.10	0.00	2.080	9.71	0.00	2.137	10.20	0.00
17	1.867	9.63	0.00	1.646	8.92	0.00	1.687	8.17	0.00
Avg.	1.689	8.73	0.02	1.632	8.40	0.29	1.683	8.82	0.01

CS	Bishop			UpliftVan			Spencer		
Dike section (#)	**Stab. factor (-)**	**Reliability Index (-)**	**$P_{failure}$ (%)**	**Stab. factor (-)**	**Reliability Index (-)**	**$P_{failure}$ (%)**	**Stab. factor (-)**	**Reliability Index (-)**	**$P_{failure}$ (%)**
2	1.357	5.63	0.00	1.367	5.95	0.00	1.426	6.31	0.00
2a	1.070	1.16	12.30	1.071	1.15	12.50	1.036	0.61	27.00
3	1.331	3.87	0.01	1.276	4.59	0.00	1.332	4.41	0.00
4	1.295	4.27	0.00	1.276	4.04	0.00	1.292	4.48	0.00
5	1.070	0.85	19.80	1.005	0.00	50.50	1.070	0.93	17.60
6	1.189	3.25	0.06	1.173	3.13	0.09	1.205	3.80	0.01
6a	1.288	4.94	0.00	1.275	4.55	0.00	1.270	4.42	0.00
7	1.435	6.72	0.00	1.440	6.63	0.00	1.473	7.32	0.00
8	1.463	7.38	0.00	1.453	7.38	0.00	1.477	7.63	0.00
9	1.336	5.58	0.00	1.269	4.76	0.00	1.296	5.25	0.00
10	1.600	11.7	0.00	1.477	10.00	0.00	1.533	10.60	0.00
10a	1.117	2.54	0.56	1.060	1.11	13.30	1.014	0.22	41.30
12	1.274	6.18	0.00	1.323	5.97	0.00	1.309	6.94	0.00
14	1.450	7.96	0.00	1.459	8.98	0.00	1.505	7.52	0.00
15	1.657	7.44	0.00	1.504	6.97	0.00	1.562	7.71	0.00
17	1.554	7.61	0.00	1.365	5.95	0.00	1.430	7.28	0.00
Avg.	1.343	5.44	2.05	1.300	5.07	4.77	1.327	5.34	5.37